Inorg. Chem. **2007**, *46*, 11048–11062

Structural Diversity and Supramolecular Aggregation in Calcium, Strontium, and Barium Salicylates Incorporating 1,10-Phenanthroline and 4,4′-Bipyridine: Probing the Softer Side of Group 2 Metal Ions with Pyridinic Ligands†

Ramaswamy Murugavel* and Remya Korah

Department of Chemistry, Indian Institute of Technology-Bombay, Powai, Mumbai 400076, India

Received May 20, 2007

Group 2 metal complexes $[Ca(SA)_2(phen)]_n$ (**1**), $[Sr_2(SA)_4(phen)_4]$ (**2**), and $[Ba(SA)_2(phen)_2]_n$ (**3**) (SA = salicylate) have been obtained by the addition of 1,10-phenanthroline (phen) to the corresponding metal salicylates, while the bipyridine derivatives $\{[Ca_3(SA)_6(H_2O)_4](4bpy)_2\}_n$ (**4**), $\{[Sr(SA)_2(H_2O)_3](4bpy)_{1.5}(H_2O)\}_n$ (**5**), and $\{[Ba(SA)_2(H_2O)_3]\text{-}(4bpy)_{1.5}(H_2O)\}_n$ (**6**) have been synthesized starting from the respective metal carbonates, salicylic acid (SA–H), and 4,4′-bipyridine (4bpy). The new compounds have been characterized by elemental analysis, pH measurements, thermal analysis, and spectroscopic measurements (IR, NMR, ultraviolet, and fluorescence). Molecular structure determination by single-crystal X-ray diffraction has been carried out for all the compounds. The thermal analysis studies indicate the loss of coordinated and/or lattice water molecules below 200 °C in **4**–**6** and the absence of any coordinated or uncoordinated water molecules in compounds **1**–**3**. Compounds **1** and **3**–**6** exist as one-dimensional polymers while compound **2** crystallizes as a discrete dimer. Considerable variations have been observed in the molecular structures of **1**–**6** in terms of the geometry around the metal, the binding mode of salicylate, and the coordination behavior of the pyridine ligand. Calcium ion is hexacoordinated in **1,** while in **4** both hexa- and heptacoordinated calcium ions are simultaneously present. Strontium exhibits coordination numbers of nine and eight in **2** and **5**, respectively. The barium ions in **3** and **6** assume coordination numbers of eight and seven, respectively. While the OH group of the salicylate ligand does not directly bind the metal in **1**–**3**, it coordinates to the metal ions in complexes in **4**–**6** in the un-ionized form. The 4bpy molecules show no direct ligation to the metal in **4**–**6**; the phen ligands in **1**–**3**, however, occupy one side of the coordination sphere around the metal. The presence of additional O–H···O, C–H···O, and N–H···O hydrogen bonding and π–π stacking in these compounds results in the formation of polymeric structures. The results obtained for the calcium complexes in this study have been compared with the available data in structural calcium chemistry with the aid of a detailed analysis of the Cambridge Structural Database.

Introduction

The design and synthesis of new alkaline-earth metal complexes is an emerging area of interest owing to the potential applications of these complexes in various fields such as catalysis, material science, and biochemistry.[1−5] The fact that the group 2 chemistry, which is determined by the size and charge density of the metal ion,[6] varies considerably on moving down the group is another reason which has made

† Dedicated to Professor V. Krishnan on his 70th birthday.

* To whom correspondence should be addressed. E-mail: rmv@chem.iitb.ac.in. Fax: + 91 (22) 2572 3480.

(1) (a) Cowan, K. D. U.S. Patent 4,544767, 1985. (b) Chandler, C. D.; Roger, C.; Hampden-Smith, M. J. *Chem. Rev.* **1993**, *93*, 1205. (c) Boyle, T. J.; Bucheit, C. D.; Rodriguez, M. A.; A1-Shareef, H. N.; Hernandez, B. A.; Scott, B.; Ziller, J. W. *J. Mater. Res.* **1996**, *9*, 2246.

(2) (a) Westerhausen, M.; Schneiderbauer, S.; Kneifel, A. N.; Söltl, Y.; Mayer, P.; Nöth, H.; Zhong, Z.; Dijkstra, P. J.; Feijen, J. *Eur. J. Inorg. Chem.* **2003**, 3432. (b) Fromm, K. M.; Gueneau, E. D. *Polyhedron* **2004**, *23*, 1479.

(3) (a) Evans, C. A.; Guerremont, R.; Rabenstein, D. L. *Metal Ions in Biological Systems*; Sigel, H., Ed.; Marcel-Dekker: New York, 1979; Vol. 9, p 41. (b) Kendrick, M. J.; May, M. T.; Plishka, M. J.; Robinson, K. D. *Metals in Biological Systems;* Ellis Horwood: New York, 1992; p 57−65.

(4) Doyne, T. *Adv. Protein Chem.* **1966**, *22*, 600.

(5) Freeman, H. C. *Inorganic Biochemistry;* Eichhorn, J., Ed.; Marcel-Dekker: New York, 1979; Vol. 1, p 129.

(6) Poonia, N. S.; Bajaj, A. V. *Chem. Rev.* **1979**, *79*, 389.

10.1021/ic700977w CCC: $37.00
Published on Web 11/30/2007

the studies of these metal complexes a rapidly developing area. For example, calcium is observed to exhibit coordination numbers ranging from three to nine, although the most commonly observed are six, seven and eight.[7−23] Strontium and barium prefer coordination numbers of 6 to 12.[9b,15−19,24−27] The coordination behavior of alkaline-earth metal cations, especially that of calcium, is a topic of current interest owing to the vital roles these metal ions play in biological systems.[28] The importance of calcium in biological and structural inorganic chemistry has resulted in detailed structural analysis through the information available in the Cambridge Structural Database (CSD) and Protein Data Bank (PDB) crystal structure databases.[29,30]

Among the alkaline-earth metal complexes, the complexes formed by aromatic carboxylic acids have been widely investigated.[14,17−20,31] Recently, Fox et al.[32] have studied the reactivity of biologically relevant α-amino carboxylic acids toward calcium and shown that glycine and alanine bind to the metal using both oxygen and nitrogen donor centers. The stereochemistry of the interaction between carboxylates and calcium has also been widely studied due to its importance in protein function−structure analysis.[30,31]

The introduction of other functionalities on the aromatic ring, in addition to carboxylic groups, has produced a variety of supramolecular structures. We have recently reported on the coordination behavior of 2-aminobenzoic and related acids toward alkaline-earth metal ions.[16,20a,b] Schmidbaur,[34] Drake,[35] and others[18,20h,36] have studied the coordination behavior of salicylic acid (SA−H) toward the group 2 metal cations. Our investigations on group 2 metal complexes of thiosalicylic acid have shown that while the coordination is exclusively through the carboxylate groups in the case of calcium and strontium, the disulfide linkage of the oxidized ligand also participates in the metal binding in the case of the softer barium ion.[19]

It is well-known that the chelating ligands such as 1,10-phenanthroline (phen) and 2,2′-bipyridine may inhibit the expansion of the polymeric framework to give coordination polymers of low-dimensionality or zero-dimensional molecules. A number of transition-metal complexes of substituted and unsubstituted salicylic acids (SA−H) in the absence or presence of coordinating amines have been reported in the literature.[37,38] On the other hand, 4,4′-bipyridine (4bpy) is known to be an ideal connector between the metal atoms

(7) (a) He, X.; Noll, B. C.; Beatty, A.; Mulvey, R. E.; Henderson K. W. *J. Am. Chem. Soc.* **2004**, *126*, 7444. (b) He, X.; Allan, J. F.; Noll, B. C.; Kennedy, A. R.; Henderson, K. W. *J. Am. Chem. Soc.* **2005**, *127*, 6920. (c) Davies, R. P. *Inorg. Chem. Commun.* **2000**, *3*, 13.

(8) (a) Feil, F.; Harder, S. *Eur. J. Inorg. Chem.* **2005**, 4438. (b) Avent, A. G.; Crimmin, M. R.; Hill, M. S.; Hitchcock, P. B. *Dalton Trans.* **2005**, 278. (c) Tang, Y.; Zakharov, L. N.; Kassel, W. S.; Rheingold, A. L.; Kemp, R. A. *Inorg. Chim. Acta* **2005**, *358*, 2014.

(9) (a) Chisholm, M. H.; Gallucci, J. C.; Phomphrai, K. *Inorg. Chem.* **2004**, *43*, 6717. (b) Teng, W.; Ruhlandt-Senge, K. *Organometallics* **2004**, *23*, 952.

(10) (a) Ullström, A.-S.; Warminska, D.; Persson, I. *J. Coord. Chem.* **2005**, *58*, 611. (b) Crane, J. D.; Moreton, D. J.; Rogerson, E. *Eur. J. Inorg. Chem.* **2004**, *21*, 4237. (c) Sahbari, J. J.; Olmstead, M. M. *Acta Crystallogr., Sect. C* **1983**, *39*, 208. (d) Sohrin, Y.; Kokusen, H.; Kihara, S.; Matsui, M.; Kushi, Y.; Shiro, M. *J. Am. Chem. Soc.* **1993**, *115*, 4128.

(11) Sohrin, Y.; Matsui, M.; Hata, Y.; Hasegawa, H.; Kokusen, H. *Inorg. Chem.* **1994**, *33*, 4376.

(12) Tesh, K. F.; Burkey, D. J.; Hanusa, T. P. *J. Am. Chem. Soc.* **1994**, *116*, 2409.

(13) Perruchas, S.; Simon, F.; Uriel, S.; Avarvari, N.; Boubekeur, K.; Batail P. *J. Organomet. Chem.* **2002**, *643*−*644*, 301.

(14) (a) Starosta, W.; Ptasiewicz-bąk, H.; Leciejewicz, J. *J. Coord. Chem.* **2003**, *56*, 33 and references cited therein. (b) Hundal, G.; Martin, M.-R.; Hundal, M. S.; Poonia, N. S. *Acta Crystallogr.* **1996**, *C52*, 786. (c) Zasurskaya, L. A.; Polyakova, I. N.; Polynova, T. N.; Poznyak, A. L.; Sergienko, V. S. *Crystallogr. Rep.* **2002**, *47*, 783. (d) Wörl, S.; Fritsky, I. O.; Hellwinkel, D.; Pritzkow, H.; Krämer, R. *Eur. J. Inorg. Chem.* **2005**, *22*, 759. (e) Datta, A.; Karan, N. K.; Mitra, S.; Tiekink, E. R. T. *Polyhedron* **2002**, *21*, 2237.

(15) Reger, D. L.; Little, C. A.; Smith, M. D. *Inorg. Chem.* **2002**, *41*, 19.

(16) (a) Murugavel, R.; Karambelkar, V. V.; Anantharaman, G.; Walawalkar, M. G. *Inorg. Chem.* **2000**, *39*, 1381. (b) Murugavel, R.; Kumar, P.; Walawalkar, M. G.; Mathialagan, R. *Inorg. Chem.* **2007**, *46*, 6828.

(17) Hundal, G.; Hundal, M. S.; Obrai, S.; Poonia, N. S.; Kumar, S. *Inorg. Chem.* **2002**, *41*, 2077.

(18) Debuyst, R.; Dejehet, F.; Dekandelaer, M. C.; Declerco, J. P.; Germain, G.; Van Meerssche, M. *J. Chim. Phy.* **1979**, *78*, 1117.

(19) Murugavel, R.; Baheti, K.; Anantharaman, G. *Inorg. Chem.* **2001**, *40*, 6870.

(20) (a) Murugavel, R.; Banerjee, S. *Inorg. Chem. Commun.* **2003**, *6*, 810. (b) Murugavel, R.; Karambelkar, V. V.; Anantharaman, G. *Indian J. Chem., Sect. A* **2000**, *39A*, 843. (c) Starosta, W.; Ptasiewicz-bąk, H.; Leciejewicz, J. *J. Coord. Chem.* **2004**, *57*, 167. (d) Onoda, A.; Yamada, Y.; Nakayama, Y.; Takahashi, K.; Adachi, H.; Okamura, T.-A.; Nakamura, A.; Yamamoto, H.; Ueyama, N.; Vyprachticky, D.; Okamoto, Y. *Inorg. Chem.* **2004**, *43*, 4447. (e) Chen, X. M.; Mak, T. C. W. *Polyhedron* **1994**, *13*, 1087. (f) Cole, L. B.; Holt, E. M. *Inorg. Chim. Acta* **1989**, *I60*, 195. (g) Ueyama, N.; Takeda, J.; Yamada, Y.; Onoda, A.; Okamura, T.; Nakamura, A. *Inorg. Chem.* **1999**, *38*, 475. (h) Hundal, G.; Martin, M.-R.; Hundal, M. S.; Poonia, N. S. *Acta Crystallogr.* **1996**, *C52*, 789.

(21) Wendell, L. T.; Bender, J.; He, X.; Noll, B. C.; Henderson, K. W. *Organometallics* **2006**, *25*, 4953.

(22) Poonia, N. S.; Hundal, G.; Obrai, S.; Hundal, M. S. *Acta Crystallogr., Section C: Cryst. Struct. Commun.* **1999**, *55* (1), 26.

(23) (a) Starosta, W.; Leciejewicz, J. *J. Coord. Chem.* **2005**, *58*, 891. (b) Kumar, K.; Tweedle, M. F.; Malley, M. F.; Gougoutas, J. Z. *Inorg. Chem.* **1995**, *34*, 6472.

(24) (a) Evans, W. J.; Giarikos, D. G.; Greci, M. A.; Ziller, J. W. *Eur. J. Inorg. Chem.* **2002**, 453. (b) Clegg, W.; Hunt, P. A.; Straughan, B. P.; Mendiola, M. A. *J. Chem. Soc., Dalton Trans.* **1989**, 1127. (c) Hitzbleck, J.; Deacon, G. B.; Ruhlandt-Senge, K. *Angew. Chem., Int. Ed.* **2004**, *43*, 5218.

(25) (a) Kanters, J. A.; Smeets, W. J. J.; Venkatasubramanian, K.; Poonia, N. S. *Acta Crystallogr., Sect. C: Cryst. Struct. Commun.* **1984**, *40*, 1701. (b) Panda, T. K.; Zulys, A.; Gamer, M. T.; Roesky, P. W. *J. Organomet. Chem.* **2005**, *690*, 5078. (c) Veith, M.; Mathur, S.; Huch, V.; Decker, T. *Eur. J. Inorg. Chem.* **1998**, 1327.

(26) Waters, A. F.; White, A. H. *Aust. J. Chem.* **1996**, *49*, 27, and other related articles in this issue.

(27) Poonia, N. S.; Chhabra, N.; Sheldrick, W. S.; Hundal, G.; Obrai, S.; Hundal, M. S. *Acta Crystallogr.* **1999**, *C55*, 24.

(28) (a) Katz, A. K.; Glusker, J. P.; Beebe, S. A.; Bock, C. W. *J. Am. Chem. Soc.* **1996**, *118*, 5752. (b) Hitzbleck, J.; Deacon, G. B.; Ruhlandt-Senge, K. *Angew. Chem., Int. Ed.* **2004**, *43*, 5218.

(29) Einspahr, H.; Bugg, C. E. *Acta Crystallogr., Sect. B* **1981**, *37*, 1044.

(30) (a) Carrell, C. J.; Carrell, H. L.; Erlebacher, J.; Glusker, J. P. *J. Am. Chem. Soc.* **1988**, *110*, 8651. (b) Tunell, I.; Lim, C. *Inorg. Chem.* **2006**, *45*, 4811. (c) Pidcock, E.; Moore, G. R. *J. Biol. Inorg. Chem.* **2001**, *6* (5−6), 479. (d) Gracy, J.; Argos, P. *Bioinformatics* **1998**, *14* (2), 174.

(31) (a) Plater, M. J.; Howie, R. A.; Roberts, A. J. *Chem. Commun.* **1997**, 893. (b) Plater, M. J.; Roberts, A. J.; Marr, J.; Lachowski, E. E.; Howie, R. A. *J. Chem. Soc., Dalton Trans.* **1998**, 797. (c) Zhu, H.-F.; Zhang, Z.-H.; Sun, W.-Y.; Okamura, T.-a.; Ueyama, N. *Crys. Growth Des.* **2005**, *5* (1), 177. (d) Lewandowski, W.; Dasiewicz, B.; Koczoń, P.; Skierski, J.; Dobrosz-Teperek, K.; Świsłocka, R.; Fuks, L.; Priebe, W.; Mazurek, A. P. *J. Mol. Struct.* **2002**, *604*, 189.

(32) Fox, S.; Büsching, I.; Barklage, W.; Strasdeit, H. *Inorg. Chem.* **2007**, *46*, 818.

(33) (a) Gandour, R. D. *Bioorg. Chem.* **1981**, *10*, 169. (b) Chakrabarti, P. *Protein Eng.* **1990**, *4*, 49.

(34) Schmidbaur, H.; Kumberger, O.; Riede, J. *Inorg. Chem.* **1991**, *30*, 3101.

(35) Drake, S. R.; Anderson, K. D.; Hursthouse, M. B.; Malik, K. M. A. *Inorg. Chem.* **1993**, *32*, 1041.

(36) Helems, R.; Cole, L. B.; Holt, E. M. *Inorg. Chim. Acta* **1998**, *152*, 9.

Scheme 1. Synthesis of Complexes **1**−**6**

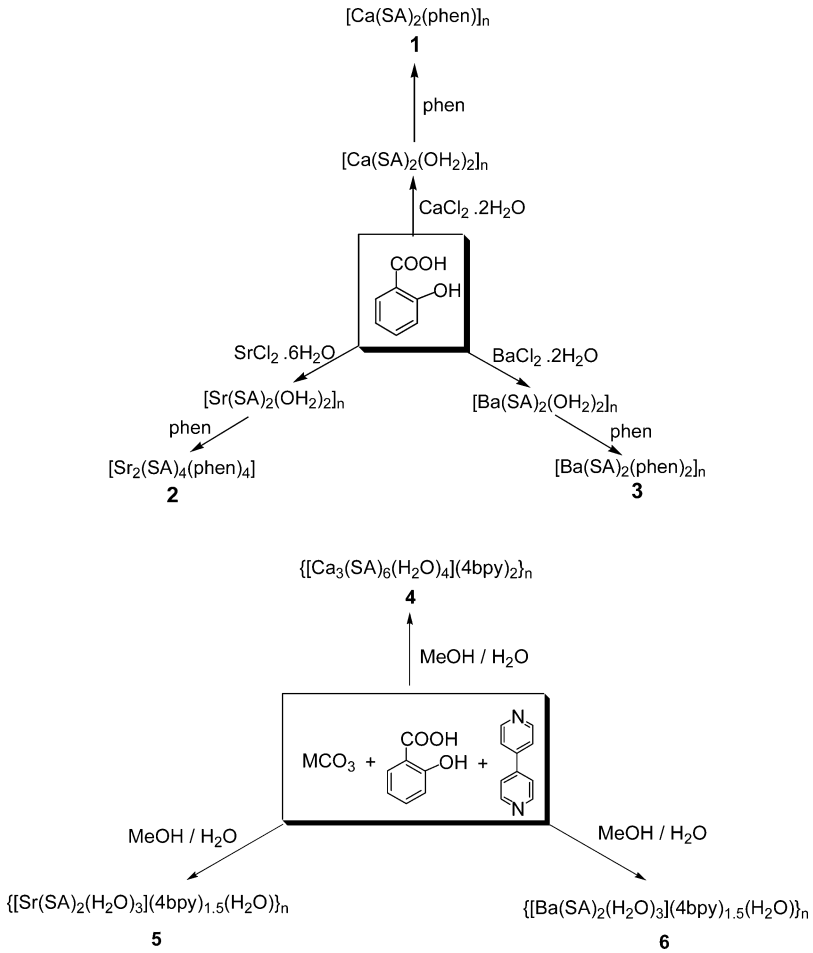

for the propagation of coordination networks, resulting in the formation of a variety of networks.[39−42] However, very little is known on the use of phen and 4bpy in group 2 metal coordination chemistry.[14e,43,44] Keeping this observation in mind, in this contribution, we report the synthesis and spectral and structural characterization of the first examples of calcium, strontium, and barium carboxylate complexes which incorporate additional chelating phen ligands; the reluctance of group 2 metal ions to bind to potentially bridging ligands such as 4bpy is also demonstrated.

Results and Discussion

Synthesis. The salicylate complexes of calcium, strontium, and barium, **1**−**3**, have been prepared from the corresponding metal salicylate precursors by treatment with phen in methanol−water at ambient temperature (Scheme 1). The precursor metal salicylate complexes have been prepared by following the literature methods, by using metal chlorides and SA−H in the presence of aqueous ammonia.[18] The new compounds **1**−**3** were found to be highly soluble in solvents such as MeOH, EtOH, and dimethylsulfoxide (DMSO).

The synthesis of 4bpy-containing compounds **4**−**6** were achieved by the treatment of the respective metal carbonates with SA−H and 4bpy in a 1:2:1 ratio in methanol (Scheme 1). All the new compounds were obtained as well-formed single crystals directly from the reaction mixture within a few days.

Analytical Data and Spectral Characterization. Complexes **1**−**6** have been obtained in a moderate to good yield (32−64%) in an analytically pure form.[45] Compounds **1**−**5** do not melt or decompose below 200 °C, while compound **6** melts around 185−190 °C. In all cases, the empirical

(37) (a) Joyave, J. L.; Steinhauer, L. S.; Dillehay, D. L.; Born, C. K.; Hamrick, M. E. *Biochem. Pharmacol.* **1985**, *34* (21), 3915−3919. (b) Kunkely, H.; Vogler, A. *Inorg. Chim. Acta* **2004**, *357*, 888. (c) Ranford, J. D.; Sadler P. J.; Tocher, D. A. *J. Chem. Soc., Dalton Trans.* **1993**, 3393. (d) Brownless, N. J.; Edwards, D. A.; Mahon, M. F. *Inorg. Chim. Acta* **1999**, *287*, 89. (e) In, Y.; Hayashi, C.; lshida T. *lnorg. Chim. Acta* **1997**, *260*, 111. (f) Devereux, M.; Curran, M.; McCann, M.; Casey, R. M. T.; Mckee, V. *Polyhedron* **1996**, *15*, 2029. (g) Pavacik, P. S.; Huffman, J. C.; Christou, G. *J. Chem. Soc., Chem. Commun.* **1986**, 43.

(38) Palanisami, N.; Prabusankar, G.; Murugavel, R. *Inorg. Chem. Commun.* **2006**, *9*, 1002.

(39) (a) Biradha, K.; Sarkar, M.; Rajput, L. *Chem. Commun.* **2006**, 4169. (b) Pothiraja, R.; Sathiyendiran, M.; Butcher, R. J.; Murugavel, R. *Inorg. Chem.* **2004**, *43*, 7585. (c) Pothiraja, R.; Sathiyendiran, M.; Butcher, R. J.; Murugavel, R. *Inorg. Chem.* **2005**, *44*, 6314.

(40) Wang, Y.-B.; Zhuang, W.-J.; Jin, L.-P.; Lu, S.-Z. *J. Mol. Struct.* **2005**, *737*, 165.

(41) He, H.-Y.; Zhou, Y.-L.; Hong, Y.; Zhu, L.-G. *J. Mol. Struct.* **2005**, *737*, 97.

(42) Sun, D.; Cao, R.; Sun, Y.; Bi, W.; Li, X.; Wang, Y.; Shi, Q.; Li, X. *Inorg. Chem.* **2003**, *42*, 7512.

(43) (a) Chowdhury, S. R.; Komiyama, T.; Yukawa, Y.; Bhattacharyya, R. *Inorg. Chem. Commun.* **2004**, *7*, 1117. (b) Yan, Z.; Day, C. S.; Lachgar, A. *Inorg. Chem.* **2005**, *44* (13), 4499. (c) Datta, A.; Hossain, G. M. G.; Karan, N. K.; Abdul Malik, K. M.; Mitra, S. *Inorg. Chem. Commun.* **2003**, *6*, 266.

(44) de Lill, D. T.; Bozzuto, D. J.; Cahill, C. L. *Dalton Trans.* **2005**, 2111.

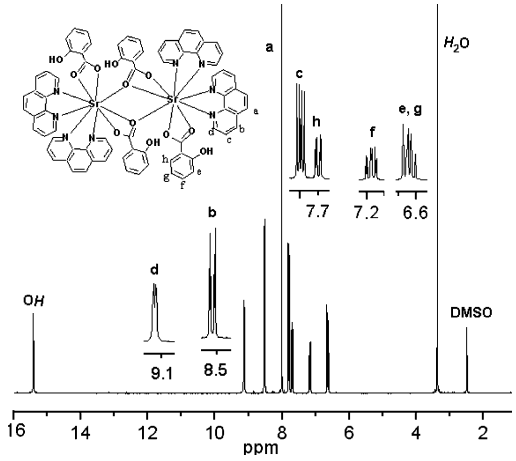

Figure 1. ^{1}H NMR spectrum of **2** in DMSO-d_6.

formula and composition of the products could easily be established from the analytical data. The infrared spectra of all the compounds recorded as KBr diluted discs showed absorption corresponding to phenolic O−H and C═O stretching vibrations. The IR spectra of phen derivatives **1**−**3** show a relatively weaker O−H stretching absorption, indicating the absence of any additional water molecules, while the relatively stronger and broader peaks around 3400−3500 cm^{-1} in the spectra of 4bpy derivatives **4**−**6** confirm the presence of water in the structure.

The ^{1}H NMR spectra for **1**−**3** in DMSO-d_6 give four signals for the phen and four more signals for the salicylate protons. The phen protons resonate at downfield compared with the salicylate protons. The resonance for the OH proton is downfield shifted in all the cases and is observed as a singlet at around 15.5 ppm. The aromatic protons appear as multiplets due to the three and four bond couplings with neighboring protons. The position and splitting pattern of salicylate ligand protons in the 4bpy complexes **4**−**6** are almost similar to those in phen complexes **1**−**3**. However, the aromatic protons from 4bpy complexes give rise to only two resonances, owing to the similarity in magnetic environments. The ^{1}H NMR spectrum of the representative example **2** is shown in Figure 1. The ^{13}C NMR spectrum of **1** shows 11 resonances while that of corresponding 4bpy complex **4** shows 10 resonances, as expected. The chemical shift values of salicylate carbons do not show much difference between phen and 4bpy complexes. In both cases, the carboxylic carbon is the most deshielded and appears at around 174 ppm.

The UV−vis spectra of compounds **1**−**3** are similar and show two major absorptions around 229 and 264 nm and a shoulder around 208 nm. The absorption maxima of free phen and SA−H appear in the ultraviolet region at 229 and 263 nm and 208, 236, and 301 nm, respectively, which are assigned to the $\pi-\pi^*$ transitions of the aromatic ring, belonging to the K band.[46] Thus, it is evident from the spectra that the UV absorption of the complexes is dominated by the absorption of phen, for the fact that the absorptions due to SA−H appears as a shoulder at 208 nm, while phen still shows its characteristic absorption peak at 264 nm. This indicates that the fluorescence properties of the complex are mainly determined by the energy transfer from phen to the M^{2+} (M = Ca, Sr, Ba) ion.[47]

The fluorescence studies of alkaline-earth metals are of considerable importance, since they are the most abundant divalent cations in living cells and play vital roles in many cellular processes. A great deal of effort has been devoted to the design and synthesis of sensitive and selective fluorescent sensors, especially for Mg^{2+} and Ca^{2+}.[48−50] The fluorescence spectra of the compounds **1**−**3** recorded in methanol solution show a similar spectral pattern. Two emission maxima are observed at around 366 and 383 nm. Similarly, the excitation spectra also contain two maxima around 270 and 293 nm. Interestingly, the emission signals of free salicylic acid appear around 402 nm, while the free phenanthroline does not show any appreciable fluorescence activity. The emission and excitation intensities of Sr and Ba complexes **2** and **3** are clearly enhanced as a result of metal coordination, while those of Ca complex **1** appear reduced compared with those of free salicylic acid. This is particularly surprising in the light of recent reports on the fluorescence enhancements of calcium carboxylate complexes.[16b] The time-resolved fluorescence lifetime measurements for compounds **1**−**3** yield similar values, falling in the range of 5.41−5.54 ns. The fluorescence spectra of the compounds **1**−**3**, SA−H, and phen are shown in Figure 2.

The absorption spectra of **4**−**6** are also similar to each other. Two major absorptions were observed around 207 and 236 nm, and a small shoulder was observed at around 305 nm. For free 4bpy, the absorption maxima appear in the ultraviolet region at 204 and 239 nm while those of free SA−H appear at 208, 236, and 301 nm. It appears that in 4bpy derivatives, the absorption is almost equally contributed by the salicylate and bipyridine ligands. Compounds **4**−**6** emit at around 400 nm (Figure 3), which matches well with the emission wavelength of free salicylic acid. However, the metal coordination causes significant alteration in intensity of fluorescence: While that of calcium compound **4** decreases as in the cases of phen complexes, the fluorescence

(45) During the synthesis of **4**, the formation a second product $[Ca(SA)_2(4bpy)_2(H_2O)_2]_n$ was observed in 10% yield. When the reaction was repeated in a 1:1.5 ratio of $CaCO_3$ and 4bpy, the yield of this increased to 23%. However, due to the poor quality of the crystals obtained, X-ray diffraction data of this compound could not be obtained.

(46) Hong, S. H. *The Application of Spectral Analysis in Organic Chemistry*; Science Publishing House: Beijing, 1981.
(47) Xu, C.-J.; Xie, F.; Guo, X.-Z.; Yang, H. *Spectrochim. Acta, Part A* **2005**, *61*, 2005.
(48) (a) Bühlmann, P.; Pretsch, E.; Bakker, E. *Chem. Rev.* **1998**, *98*, 1593. (b) Prodi, L.; Bolletta, F.; Montalti, M.; Zaccheroni, N. *Tetrahedron Lett.* **1998**, *39*, 5451. (c) Samant, R. A.; Ijeri, V. S.; Srivastava, A. K. *J. Chem. Eng. Data* **2003**, *48*, 203. (d) Gromov, S. P.; Ushakov, E. N.; Fedorova, O. A.; Baskin, I. I.; Buevich, A. V.; Andryukhina, E. N.; Alfimov, M. V.; Johnels, D.; Edlund, U. G.; Whitesell, J. K.; Fox, M. A. *J. Org. Chem.* **2003**, *68*, 6115.
(49) (a) Arunkumar, E.; Chithra, P.; Ajayaghosh, A. *J. Am. Chem. Soc.* **2004**, *126*, 6590. (b) Liu, Y.; Duan, Z.-Y.; Zhang, H.-Y.; Jiang, X.-L.; Han, J.-R. *J. Org. Chem.* **2005**, *70*, 1450.
(50) (a) Player, T. N.; Shinodam, S.; Tsukube, H. *Org. Biomol. Chem.* **2005**, *3*, 1615. (b) Vicente, M.; Bastida, R.; Lodeiro, C.; Macías, A.; Parola, A. J.; Valencia, L.; Spey, S. E. *Inorg. Chem.* **2003**, *42*, 6768. (c) Kawakami, J.; Fukushi, A.; Ito, S. *Chem. Lett.* **1999**, 955 (d) Prodi, L.; Bolletta, F.; Zaccheroni, N.; Watt, C. I. F.; Mooney, N. J. *Chem.—Eur. J.* **1998**, *4* (6), 1090.

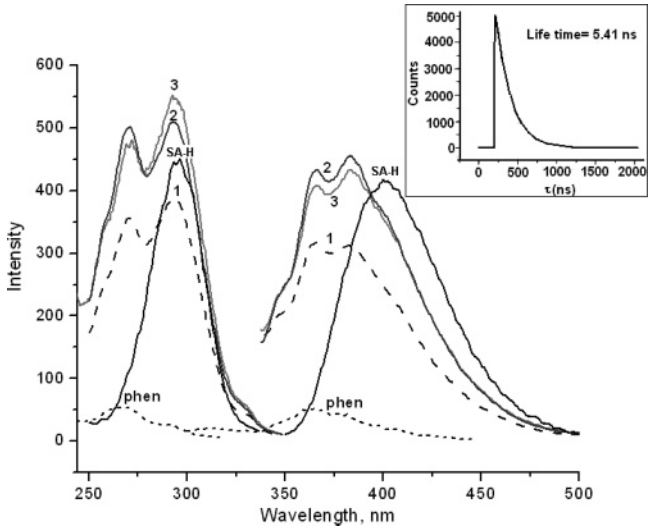

Figure 2. Excitation (left) and emission (right (λ_{ex} = 264 nm)) spectra of compounds **1**−**3**, SA−H, and phen in a 10^{-6} M MeOH solution. Inset: fluorescence decay profile of **1** (λ_{ex} = 295 nm).

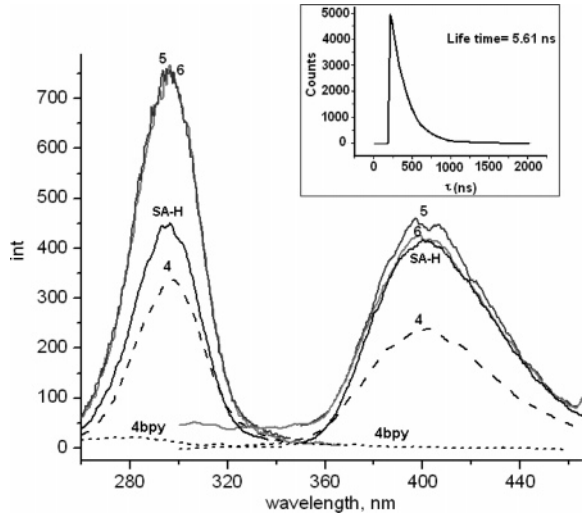

Figure 3. Excitation (left) and emission (right (λ_{ex} = 236 nm)) spectra of compounds **4**−**6**, SA−H, and 4bpy in a 10^{-6} M MeOH solution. Inset: fluorescence decay profile of **4** (λ_{ex} = 295 nm).

intensity is enhanced for strontium (**5**) and barium (**6**) derivatives. The time-resolved fluorescence lifetime measurements for compounds **4**−**6** are comparable to those of **1**−**3** (5.61 ns for **4,** 5.54 ns for **5**, and 5.51 ns for **6**) (inset of Figure 3).

Molecular Structure of Compounds 1−**6.** In order to have a clear understanding of the structures of these compounds, detailed single-crystal X-ray structural investigations have been carried out. This is especially important in the case of group 2 metal ion complexes since in most cases the solution structure is very different from the one obtained in the solid state. ^{1}H NMR correlation spectroscopy (COSY) alongwith solid-state UV−vis and fluorescence spectroscopy of the products clearly show that the solution structure is different from the solid-state structures in complexes **1**−**6** (see the Supporting Information).

Single-crystal X-ray diffraction studies reveal that all the compounds exhibit interesting structural variations in terms of coordination number and geometry around the metal ion

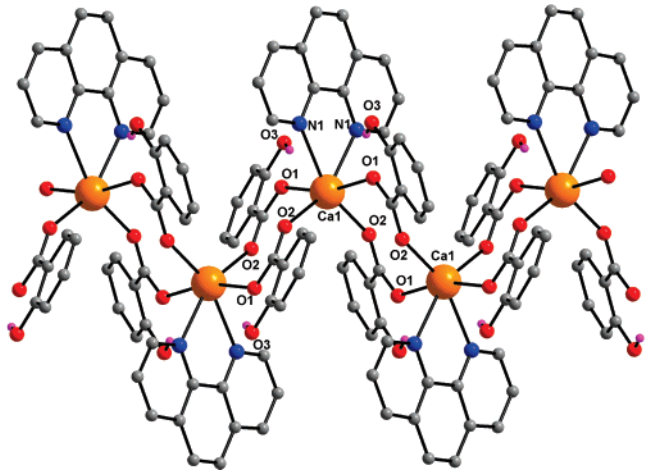

Figure 4. Molecular structure of **1**. Selected bond distances (Å) and angles (deg): Ca(1)−O(2) 2.243(3), Ca(1)−O(2)#1 2.243(3), Ca(1)−O(1) 2.362(3), Ca(1)−O(1)#1 2.362(3), Ca(1)−N(1) 2.504(4), Ca(1)−N(1)#1 2.504(4); O(2)−Ca(1)−O(2)#1 112.3(2), O(2)−Ca(1)−O(1)#1 90.0(1), O(2)−Ca(1)−O(1) 98.2(1), O(2)#1−Ca(1)−O(1)#1 98.2(1), O(2)#1−Ca(1)−O(1) 90.0(1), O(1)#1−Ca(1)−O(1) 165.5(2), O(2)−Ca(1)−N(1)#1 91.0(1), O(2)#1−Ca(1)−N(1)#1 156.8(1), O(1)#1−Ca(1)−N(1)#1 79.0(1), O(1)−Ca(1)−N(1)#1 88.8(1), O(2)−Ca(1)−N(1) 156.8(1), O(2)#1−Ca(1)−N(1) 91.0(1), O(1)#1−Ca(1)−N(1) 88.8(1), O(1)−Ca(1)−N(1) 79.0(1), N(1)#1−Ca(1)−N(1) 66.0(2). Symmetry transformations used to generate equivalent atoms: #1, $-x + {}^1/_2$, y, $-z + 1$; #2, $-x$, $-y + 1$, $-z + 1$.

as well as in the binding mode of the ligand. It is interesting to observe that, by the influence of added pyridinic co-ligand, the resulting compounds exhibit wide diversity in their structures, which also differ considerably from the complexes formed in the absence of co-ligands. The M−O[10−20,30−32] and M−N[27,51−56] bond lengths observed in all the compounds (**1**−**6**) are in good agreement with the literature values. The detailed crystal structure description for each compound is given below.

[Ca(SA)$_2$(phen)]$_n$ (1). Compound **1** crystallizes in the centrosymmetric orthorhombic space group *Pnab*. The calcium ion is hexacoordinated, being bonded to the nitrogen atoms of a phenanthroline ligand and to one carboxylate oxygen from each of the four different salicylate (2-hba) ligands around the metal ion. Each carboxylate group coordinates to a pair of neighboring calcium atoms in an asymmetric syn−anti bridging mode (Figure 4). The coordination geometry around Ca is that of distorted octahedral. Salicylate ligand coordinates to the metal center in a bridging mode to form a one-dimensional zigzag chain. The compound [Mn(SA)$_2$(2bpy)]·H$_2$O, in which Mn atoms were bridged by salicylate ligands, also forms a zigzag chain.[37f]

Two out of the four bridging salicylic oxygen atoms O(2) and O(2′) are in the same plane with the phenanthroline ligand while the other two oxygen atoms coordinate from a

(51) Drozdov, A.; Troyanov, S. *Polyhedron* **1993**, *12*, 2973.
(52) Datta, A.; Golzar Hossain, G. M.; Karan, N. K.; Malik, K. M. A.; Mitra, S. *Inorg. Chem. Commun.* **2003**, *6*, 658.
(53) Marchetti, F.; Pettinari, C.; Pettinari, R.; Cingolani, A.; Drozdov, A.; Troyanov, S. *J. Chem. Soc., Dalton Trans.* **2002**, 2616.
(54) Shen, Y.; Pan, Y.; Dong, G.; Sun, X.; Huang, X. *Polyhedron* **1998**, *7* (1), 69.
(55) Yan, Z.; Day, C. S.; Lachgar, A. *Inorg. Chem.* **2005**, *44*, 4499.
(56) Pettinari, C.; Marchetti, F.; Cingolani, A.; Leonesi, D.; Troyanov, S.; Drozdov, A. *J. Chem. Soc., Dalton Trans.* **1999**, 1555.

Table 1. Hydrogen Bond Lengths (Å) and Angles (deg) in **1**−**3**

D−H···A	D−H, Å	H···A, Å	D···A, Å	∠DHA, deg
		1		
O(3)−H(3)···O(1)	0.85(5)	1.77(5)	2.53(1)	147(5)
C(13)−H(13)···O(3)[a]	0.85(4)	2.57(4)	3.37(1)	155(4)
C(16)−H(16)···O(3)	0.97(4)	2.86(4)	3.70(1)	148(3)
C(5)−H(5)···O(3)[b]	0.96(7)	2.46(7)	3.40(1)	167(5)
		2		
O(3)−H(3A)···O(1)	0.88(3)	1.72(3)	2.543(2)	155(3)
O(6)−H(6B)···O(5)	0.91(3)	1.69(3)	2.542(2)	155(3)
C(15)−H(15)···O(2)[c]	0.96(2)	2.51(3)	3.456(3)	169(2)
		3		
O(3)−H(3)···O(2)	0.73(4)	1.88(4)	2.572(4)	159(5)
C(13)−H(13)···O(3)[d]	0.90(5)	2.57(5)	3.463(5)	171(4)

[a] Equivalent positions: $x + 1/2, -y, +z$. [b] Equivalent positions: $x - 1/2, -y + 1/2, -z + 1/2$. [c] Equivalent positions: $-x + 1, -y + 2, -z + 1$. [d] Equivalent positions: $-x + 1/2, +y - 1/2, -z - 1/2$.

plane perpendicular to this, thus forming a distorted octahedron around calcium. The phenanthroline ligand makes an N(2)−Ca(1)−N(3) angle of 66.142(2)°. The Ca−O distances range from 2.2455(1) to 2.3639(2) Å. The longer distances are those due to axial O atoms, while the shorter distances are due to equatorial carboxylate oxygen atoms trans to the nitrogen atoms. The presence of phenolic and carboxylate functionalities results in the formation of large number of intramolecular O−H···O and intermolecular C−H···O hydrogen bonds in the structure (Table 1). The C−H···O hydrogen bonds link the different layers of the one-dimensional coordination polymers into a three-dimensional network, which results in a supramolecular architecture. The packing diagram of **1** along the *a* and *b* axes is shown in Figure 5.

$[Sr_2(SA)_4(phen)_4]$ (2). The molecular structure of **2**, which crystallizes in triclinic space group $P\bar{1}$ consists of centrosymmetric dimeric molecules of $[Sr_2(SA)_4(phen)_4]$. The coordination environment of the strontium ion is filled by four nitrogen atoms from two phenanthroline ligands and five oxygen atoms (two from a chelating carboxylate and three from two tridentate carboxylates). The nine-coordinated strontium ions exhibit a distorted monocapped square antiprismatic geometry (Figure 6). Unlike in compound **1**, where the carboxylate group binds to the metal using only one kind of binding mode, in compound **2** the salicylate ligands exhibit two kinds of binding modes. Out of the two carboxylate groups on each strontium ion, one acts purely as chelating, while the other bridges the two strontium atoms in addition to the chelation, thus acting as a tridentate ligand.

The five Sr−O and four Sr−N bond lengths are quite different. The Sr−O bond lengths range from 2.609(2) to 2.680(2) Å, while Sr−N bond lengths range from 2.738(2) to 2.824(2) Å. The molecular structure of **2** showing the intramolecular hydrogen bonding is shown in Figure 7. The phenolic group of SA ligand does not take part in any kind of interaction with the metal as in the case of **1** but takes part in intramolecular hydrogen bonding with carboxylate oxygen atom O(1) (Table 1). The carboxylate oxygen atom O(2) takes part in weaker C−H···O hydrogen bonds with hydrogen atoms from an adjacent phenanthroline group.

$[Ba(SA)_2(phen)_2]_n$ (3). The molecular structure of **3** is similar to the calcium compound **1**, except that the coordination sphere of compound **3** consists of an additional phenanthroline ligand (Figure 8). This may be attributed to the larger size of the Ba ion compared with that of the Ca ion. The coordination behavior of salicylate ligand is same as that in **1**.

The coordination environment around the barium ion is of distorted bicapped octahedral, which is less common for barium (Figure 6). The carboxylate oxygen atoms O(2) from two bridging ligands occupy the axial position of the bicapped octahedra, while the other carboxylate oxygens O(1) along with two nitrogen atoms N(1) and N(2) from two different phenanthroline ligands form the equatorial

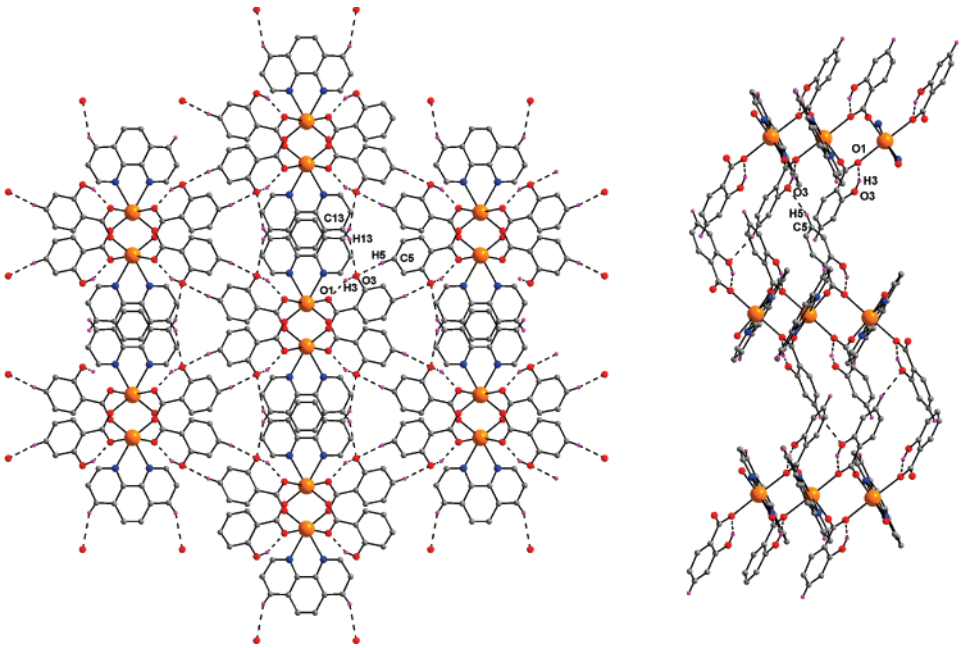

Figure 5. Hydrogen-bonding pattern of **1** (left) viewed along *a* axis and (right) viewed along *b* axis.

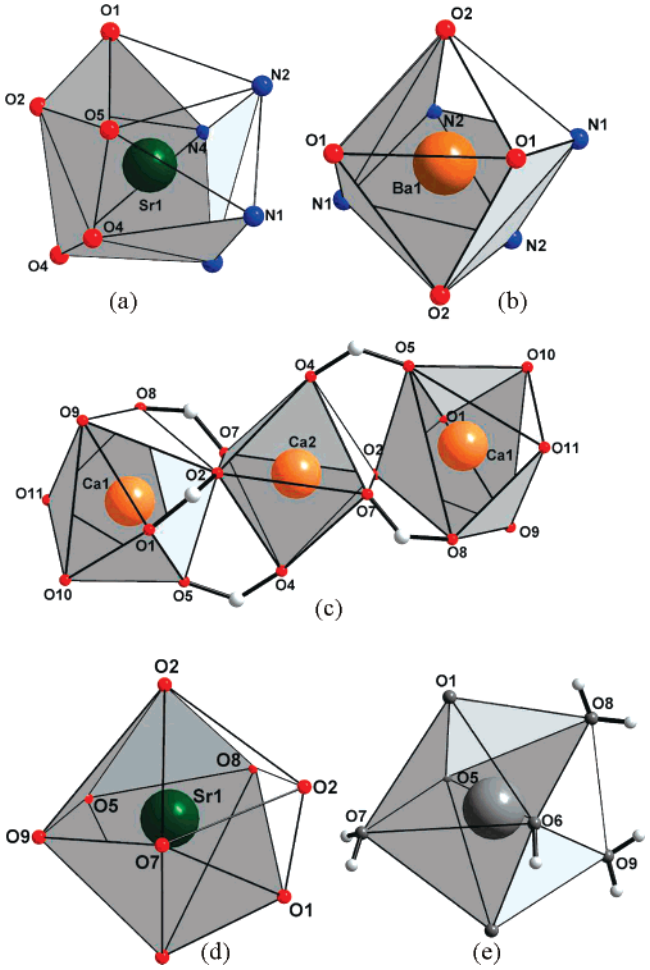

Figure 6. Coordination polyhedron of (a) **2**, (b) **3**, (c) **4**, (d) **5**, and (e) **6**.

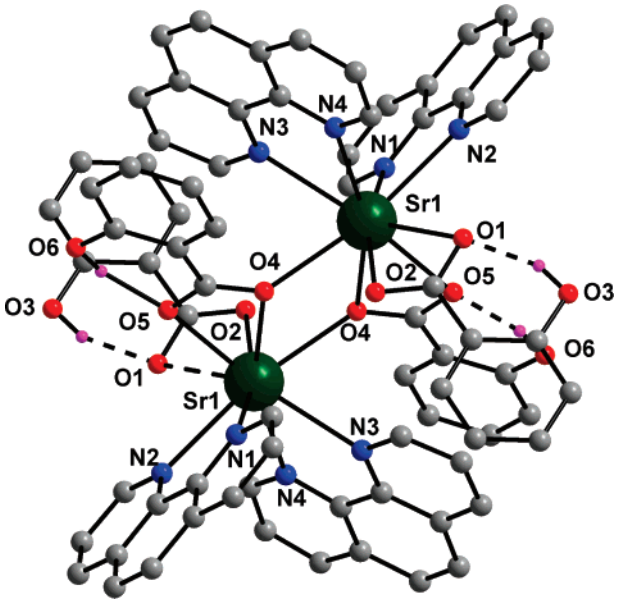

Figure 7. Molecular structure of **2**. Selected bond distances (Å) and angles (deg): Sr(1)−O(5) 2.609(2), Sr(1)−O(2) 2.618(2), Sr(1)−O(4) 2.648(1), Sr(1)−O(4)#1 2.680(2), Sr(1)−N(4) 2.738(2), Sr(1)−O(1) 2.753(2), Sr(1)−N(3) 2.761(2), Sr(1)−N(2) 2.814(2), Sr(1)−N(1) 2.824(2), O(4)−Sr(1)#1 2.680(2); O(5)−Sr(1)−O(2) 86.26(5), O(5)−Sr(1)−O(4) 49.90(4), O(2)−Sr(1)−O(4) 97.47(5), O(5)−Sr(1)−O(4)#1 107.12(6), O(2)−Sr(1)−O(4)#1 67.88(5), O(4)−Sr(1)−O(4)#1 67.04(6), O(5)−Sr(1)−N(4) 149.18(4), O(2)−Sr(1)−N(4) 85.82(5), O(4)−Sr(1)−N(4) 160.90(4), O(4)#1−Sr(1)−N(4) 97.30(6), O(5)−Sr(1)−O(1) 70.20(5), O(2)−Sr(1)−O(1) 48.67(5), O(4)−Sr(1)−O(1) 113.97(5), O(4)#1−Sr(1)−O(1) 116.49(4), N(4)−Sr(1)−O(1) 82.31(5), O(5)−Sr(1)−N(3) 146.90(5), O(2)−Sr(1)−N(3) 119.31(6), O(4)−Sr(1)−N(3) 102.67(5), O(4)#1−Sr(1)−N(3) 68.91(5), N(4)−Sr(1)−N(3) 60.01(5), O(1)−Sr(1)−N(3) 142.15(5), O(5)−Sr(1)−N(2) 81.53(6), O(2)−Sr(1)−N(2) 119.66(5), O(4)−Sr(1)−N(2) 116.85(5), O(4)#1−Sr(1)−N(2) 169.44(4), N(4)−Sr(1)−N(2) 76.72(6), O(1)−Sr(1)−N(2) 71.75(5), N(3)−Sr(1)−N(2) 100.53(6), O(5)−Sr(1)−N(1) 77.19(5), O(2)−Sr(1)−N(1) 163.45(4), O(4)−Sr(1)−N(1) 71.81(5), O(4)#1−Sr(1)−N(1) 116.78(5), N(4)−Sr(1)−N(1) 108.50(5), O(1)−Sr(1)−N(1) 123.35(5), N(3)−Sr(1)−N(1) 76.12(6), N(2)−Sr(1)−N(1) 58.39(5). Symmetry transformations used to generate equivalent atoms: #1, $-x+1$, $-y+2$, $-z+1$.

positions. The remaining two nitrogen atoms form the two caps of the bicapped octahedron. Two phenanthroline ligands bind the metal from same side and are roughly parallel to each other. The salicylate ligand bridges two metal centers using its carboxylate oxygens O(1) and O(2), resulting in the formation of the polymeric chain. In addition to the intramolecular hydrogen bond formation with the carboxylate oxygen O(2), the phenolic group forms intermolecular C−H···O bonds with neighboring layers (Table 1 and Figure 9).

The bond angles around the barium vary from 55.26(7)° to 171.88(10)°. Similarly, the Ba−O distances also vary from 2.668(2) to 2.995(3) Å. The longer distances are those due to axial O atoms, while the shorter distances are due to equatorial carboxylate oxygen atoms.

$[Ca_3(SA)_6(4bpy)_2(H_2O)_4]_n$ (4). The compound **4** crystallizes in the triclinic space group $P\bar{1}$. The compound forms a one-dimensional coordination polymeric structure with repeating units of $[Ca_3(SA)_6(H_2O)_4](4bpy)_2]$, where the backbone of the chain is formed by repeating trimeric units $[Ca_3(SA)_6(H_2O)_4]$; the 4bpy molecules are held in the lattice voids by a combination of hydrogen bonding and $\pi-\pi$ stacking interaction and are not involved in metal coordination. For every Ca_3 unit, two molecules of bipyridine molecules are present. The molecular structure of **4** showing the immediate coordination environment around the metal ion is shown in Figure 10. The coordination number and geometry around the metal ion as well as the binding mode of the salicylate ligand in **4** differs from that in **1**. Two different coordination numbers are observed for calcium in **4**: heptacoordinated Ca(1) with a distorted pentagonal bipyramidal geometry and hexacoordinated Ca(2) with a distorted octahedral geometry. The salicylate ligand exhibits three types of binding modes. The three calcium centers in each trimeric unit are connected by two bidentate bridging ligands using the carboxylate oxygen atoms O(4) and O(5). The carboxylate oxygen atoms O(4) occupy the axial positions of the octahedron. Furthermore, two tridentate ligands, which bind to the Ca(1) atom in chelating mode (using oxygens O(1) and O(2)), also bridge Ca(2) using O(2). The third binding comes from another set of two tridentate ligands, which bind Ca(1) and Ca(2) of the trimeric unit using the bridging oxygen atoms O(7) and O(8) on one hand and Ca(1) and Ca(1) of two adjacent trimeric units on the other, using the phenolic oxygen atom O(9). The bridging via the undissociated phenolic group helps in the propagation of the polymeric network by connecting the trimeric units together. One of the axial positions of the pentagonal bipyramid is

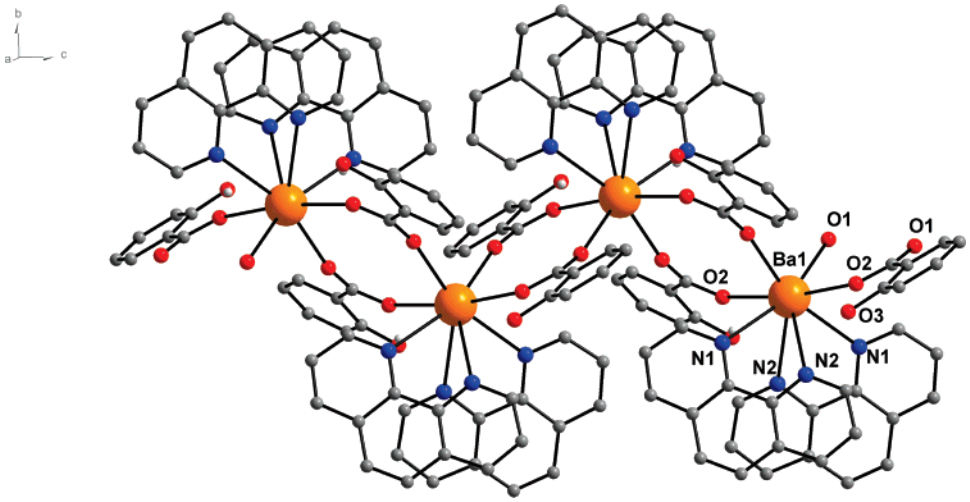

Figure 8. One-dimensional polymeric chain in **3** (viewed along *a* axis). Selected bond distances (Å) and angles (deg): Ba(1)−O(1)#1 2.668(2), Ba(1)−O(1) 2.668(2), Ba(1)−O(2)#2 2.746(2), Ba(1)−O(2)#3 2.746(2), Ba(1)−N(1) 2.927(3), Ba(1)−N(1)#1 2.927(3), Ba(1)−N(2) 2.995(3), Ba(1)−N(2)#1 2.995(3); O(1)#1−Ba(1)−O(1) 92.15(1), O(1)#1−Ba(1)−O(2)#2 88.17(7), O(1)−Ba(1)−O(2)#2 86.20(7), O(1)#1−Ba(1)−O(2)#3 86.20(7), O(1)−Ba(1)−O(2)#3 88.17(7), O(2)#2−Ba(1)−O(2)#3 171.98(0), O(1)#1−Ba(1)−N(1) 161.55(8), O(1)−Ba(1)−N(1) 75.77(8), O(2)#2−Ba(1)−N(1) 104.49(7), O(2)#3−Ba(1)−N(1) 79.71(8), O(1)#1−Ba(1)−N(1)#1 75.77(8), O(1)−Ba(1)−N(1)#1 161.55(8), O(2)#2−Ba(1)−N(1)#1 79.71(8), O(2)#3−Ba(1)−N(1)#1 104.49(7), N(1)−Ba(1)−N(1)#1 119.2(1), O(1)#1−Ba(1)−N(2) 143.19(7), O(1)−Ba(1)−N(2) 112.19(7), O(2)#2−Ba(1)−N(2) 67.30(7), O(2)#3−Ba(1)−N(2) 120.40(7), N(1)−Ba(1)−N(2) 55.26(7), N(1)#1−Ba(1)−N(2) 73.21(8), O(1)#1−Ba(1)−N(2)#1 112.19(7), O(1)−Ba(1)−N(2)#1 143.19(7), O(2)#2−Ba(1)−N(2)#1 120.40(7), O(2)#3−Ba(1)−N(2)#1 67.30(7), N(1)−Ba(1)−N(2)#1 73.21(8), N(1)#1−Ba(1)−N(2)#1 55.26(7), N(2)−Ba(1)−N(2)#1 63.9(1). Symmetry transformations used to generate equivalent atoms: #1, $-x+1$, y, $-z+{}^1/_2$; #2, x, $-y+1$, $z+{}^1/_2$; #3, $-x+1$, $-y+1$, $-z$.

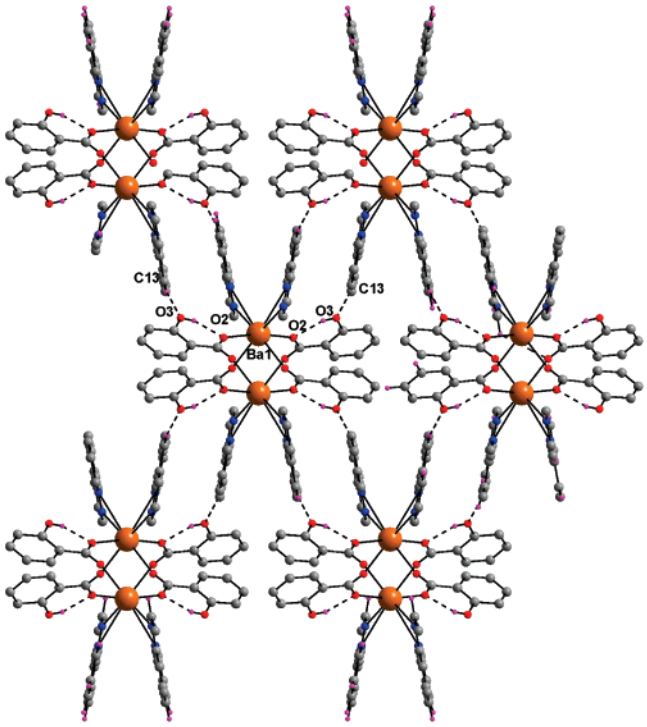

Figure 9. Hydrogen-bonding pattern in **3** when viewed along *c* axis.

occupied by a bridging carboxylate oxygen atom O(5) and the other by the phenolic oxygen atom O(9). The five equatorial positions are occupied by three carboxylate oxygens and two water oxygens (Figure 6). The coordination sphere of the heptacoordinated calcium ions (Ca(1)) consists of two bidentate and one tridentate carboxylate ligands and two water molecules each. The seventh coordination site is occupied by the hydroxyl oxygen atom from the neighboring unit. The coordination site of six-coordinated calcium does not contain any water molecules.

The two water molecules on Ca(1) are involved in extensive inter- and intramolecular hydrogen bonding with phenolic as well as carboxylic oxygen atoms. The phenolic oxygen atom also forms an intramolecular hydrogen bond with carboxylate oxygen. The two bipyridine units occupy the position near each Ca(1) center and are held using O−H···N hydrogen bonds (O(10)−H(10B)···N(1) and O(11)−H(11B)···N(2), with coordinated water molecules (Table 2). Thus, the presence of the coordinated water molecules along with the undissociated phenolic group results in the formation of a large number of intra- and intermolecular hydrogen bonds, giving rise to a three-dimensional supramolecular architecture (Figure 11).

$\{[Sr(SA)_2(H_2O)_3](4bpy)_{1.5}(H_2O)\}_n$ (5). Compound **5** forms a one-dimensional coordination polymer consisting of $\{[Sr_2(SA)_4(H_2O)_6](4bpy)_3(H_2O)_2\}$ repeating units (Figure 12). As in **4**, the 4bpy units are not coordinated to the metal and are held in the lattice by a combination of hydrogen bonding and $\pi-\pi$ interactions. Out of the four water molecules in the asymmetric part, only three are coordinated to the metal, and the fourth one occupies the lattice voids. The strontium ion is octacoordinated with a distorted monocapped pentagonal bipyramidal geometry (Figure 6).

The Sr_2 units are linked together by two tridentate bridging salicylate ligands, which chelate to one of the strontium ions through O(1) and O(2) and bridge the other using O(2). Each Sr_2 unit is connected to the neighboring units using the phenolic oxygen O(3). Thus, the chelating oxygen atoms O(1) and O(2), bridging oxygen atom O(2), bridging phenolic oxygen O(3), and three water oxygens O(7)w, O(8)w, and O(9)w fill seven of the eight coordination sites of each strontium ion. The eighth coordination site on the metal is occupied by a monodentate SA ligand, via the carboxylate oxygen atom O(5). The bridging carboxylate oxygen atom

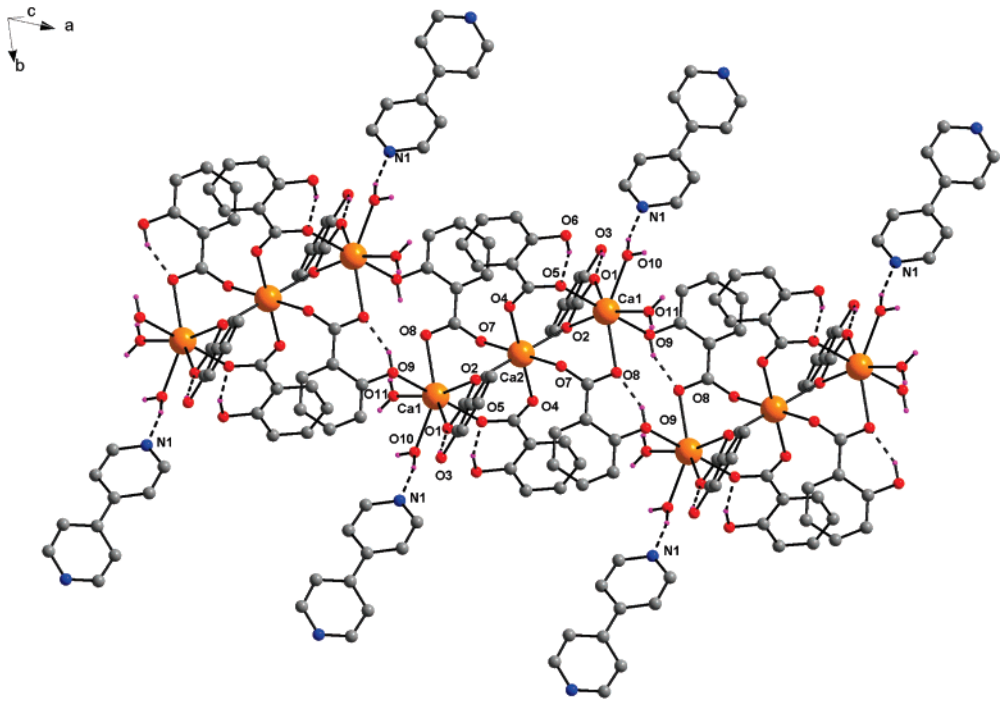

Figure 10. Molecular structure of **4**. Selected bond distances (Å) and angles (deg): Ca(1)−O(5) 2.319(1), Ca(1)−O(11) 2.368(2), Ca(1)−O(10) 2.369(2), Ca(1)−O(9) 2.436(1), Ca(1)−O(8) 2.485(1), Ca(1)−O(1) 2.495(1), Ca(1)−O(2) 2.539(1), Ca(2)−O(7) 2.280(1), Ca(2)−O(7)#1 2.280(1), Ca(2)−O(4)#1 2.309(1), Ca(2)−O(4) 2.309(1), Ca(2)−O(2)#1 2.349(1), Ca(2)−O(2) 2.349(1); O(5)−Ca(1)−O(11) 102.42(6), O(5)−Ca(1)−O(10) 79.19(5), O(11)−Ca(1)−O(10) 71.00(6), O(5)−Ca(1)−O(9) 169.30(5), O(11)−Ca(1)−O(9) 87.46(5), O(10)−Ca(1)−O(9) 100.54(5), O(5)−Ca(1)−O(8) 116.37(5), O(11)−Ca(1)−O(8) 74.97(5), O(10)−Ca(1)−O(8) 145.04(5), O(9)−Ca(1)−O(8) 69.86(5), O(5)−Ca(1)−O(1) 91.17(5), O(11)−Ca(1)−O(1) 137.25(5), O(10)−Ca(1)−O(1) 72.16(5), O(9)−Ca(1)−O(1) 78.67(5), O(8)−Ca(1)−O(1) 133.88(4), O(5)−Ca(1)−O(2) 88.65(4), O(11)−Ca(1)−O(2) 164.50(5), O(10)−Ca(1)−O(2) 122.40(5), O(9)−Ca(1)−O(2) 82.47(4), O(8)−Ca(1)−O(2) 90.46(4), O(1)−Ca(1)−O(2) 51.84(4), O(10)−Ca(1)−O(7) 150.29(5), O(9)−Ca(1)−O(7) 108.37(4), O(8)−Ca(1)−O(7) 47.29(4), O(1)−Ca(1)−O(7) 119.69(4), O(2)−Ca(1)−O(7) 69.38(4), O(7)−Ca(2)−O(7)#1 180.00(6), O(7)−Ca(2)−O(4)#1 85.30(5), O(7)#1−Ca(2)−O(4)#1 94.70(5), O(7)−Ca(2)−O(4) 94.70(5), O(7)#1−Ca(2)−O(4) 85.30(5), O(4)#1−Ca(2)−O(4) 180.000(1), O(7)−Ca(2)−O(2)#1 95.43(5), O(7)#1−Ca(2)−O(2)#1 84.57(5), O(4)#1−Ca(2)−O(2)#1 86.14(5), O(4)−Ca(2)−O(2)#1 93.86(5), O(7)−Ca(2)−O(2) 84.57(5), O(7)#1−Ca(2)−O(2) 95.43(5), O(4)#1−Ca(2)−O(2) 93.86(5), O(4)−Ca(2)−O(2) 86.14(5), O(2)#1−Ca(2)−O(2) 180.000(1), O(7)−Ca(2)−Ca(1)#1 130.49(4). Symmetry transformations used to generate equivalent atoms: #1, $-x+2$, $-y$, $-z+1$.

O(2) and the phenolic oxygen O(3) form the axis of the pentagonal bipyramid with a O(2)−Sr−O(3) angle of 172.12°, while the chelating oxygen atom O(2), the water oxygen atoms O(7), O(8), and O(9) and the terminal carboxylate oxygen O(5) occupy the five equatorial positions. The cap position is occupied by the carboxylate oxygen atom O(1). The coordination through the bridging phenolic group generates a 12-membered ring consisting of strontium, carbon, and oxygen atoms. Apart from the metal coordination, the phenolic group is also involved in the formation of inter- and intramolecular hydrogen bonds with the carboxylate oxygen atom O(1) and bipyridine groups.

There are three molecules of bipyridine corresponding to each Sr_2 unit. One molecule of bipyridine is held near each strontium center through O−H···N hydrogen bonds with coordinated and uncoordinated water molecules (Table 2). The other molecules are held in-between the layers of the one-dimensional chain and are held by hydrogen bonds with a coordinated water molecule (O(7)−H(7B)···N(2)). Bipyridine groups are arranged parallel to each other in the crystal voids. The formation of hydrogen bonds in **5** is shown in Figure 13.

$\{[Ba(SA)_2(H_2O)_3](4bpy)_{1.5}(H_2O)\}_n$ (6). Although the molecular formula of compound **6** is similar to that of **5**, the molecular structure is considerably different in terms of coordination number of the metal ion as well as binding geometry of the ligand. The barium atoms are heptacoordinated with distorted pentagonal bipyramidal geometry. Similar to **4** and **5**, compound **6** is also a one-dimensional coordination polymer, consisting of repeating units of $[Ba_2(SA)_4(H_2O)_6](4bpy)_3(H_2O)_2$ (Figure 14). The larger Ba ion in **6** has a lower coordination number than Sr in **5**, and to the best of our knowledge, such an observation is uncommon for the complexes formed by these ions from the same set of ligands.

In **5**, the Sr_2 units are linked by two tridentate bridging salicylate ligands, while the Ba_2 units in **6** are linked by two bidentate bridging ligands. These bidentate ligands coordinate through the carboxylate oxygen atoms, forming an eight-membered ring involving Ba, O, and C atoms. The axis of the pentagonal bipyramid is formed by the bridging carboxylate oxygen atom O(5) and by bridging phenolic oxygen atom O(6). The carboxylate oxygens O(4) and O(1) and the three water oxygens O(7), O(8), and O(9) occupy the equatorial positions (Figure 6). The coordination as well as the hydrogen-bonding properties of the phenolic group is similar to that in the case of **5**.

The uncoordinated water molecules are held in the lattice by the formation of multiple hydrogen bonds with coordinated water molecules and noncoordinated carboxylate oxygen atom O(2). Two of the coordinated water molecules on each barium ion form intramolecular hydrogen bonds with

Table 2. Hydrogen Bond Lengths (Å) and Angles (deg) in **4**−**6**

D−H···A	D−H, Å	H···A, Å	D···A, Å	∠DHA, deg
		4		
O(3)−H(3A)···O(1)	0.93(3)	1.683(3)	2.543(2)	152(3)
O(10)−H(10B)···N(1)	0.93(2)	1.848(2)	2.749(2)	164(2)
O(6)−H(6A)···O(5)[a]	0.91(3)	1.644(3)	2.507(2)	157(3)
O(9)−H(9A)···O(8)[b]	0.87(3)	1.723(3)	2.525(2)	152(3)
O(11)−H(11A)···O(6)[c]	0.80(3)	2.168(2)	2.914(2)	156(3)
O(10)−H(10A)···O(6)[c]	0.79(3)	2.075(3)	2.858(2)	173(3)
O(11)−H(11B)···N(2)[d]	0.87(3)	1.88(3)	2.723(2)	162(3)
		5		
O(3)−H(3A)···O(1)	0.76(3)	1.82(3)	2.549(2)	160(4)
O(6)−H(6A)···O(5)	0.70(3)	1.89(3)	2.557(3)	157(3)
O(7)−H(7A)···O(10)	0.92(5)	1.99(5)	2.909(3)	177(5)
O(7)−H(7B)···N(2)	0.74(3)	2.03(3)	2.758(3)	167(4)
O(9)−H(9A)···O(10)	0.89(4)	2.12(4)	2.876(3)	153(4)
C(7)−H(7)···O(4)	0.89(3)	2.87(3)	3.570(3)	137 (3)
C(7)−H(7)···O(5)	0.89(3)	2.66(3)	3.487(3)	155(3)
C(29)−H(29)···O(9)[e]	0.82(4)	3.00(4)	3.737(4)	151(3)
C(29)−H(29)···O(10)[e]	0.82(4)	2.80(4)	3.499(4)	144 (3)
O(8)−H(8B)···O(7)[f]	0.75(4)	2.21(4)	2.956(4)	175(4)
C(26)−H(26)···O(10)[f]	0.82(4)	2.91(4)	3.611(4)	145 (4)
O(9)−H(9B)···O(4)[f]	0.87(4)	1.84(4)	2.698(3)	166(4)
C(24)−H(24)···O(6)[g]	0.87(4)	2.76(4)	3.628(4)	176 (3)
C(4)−H(4)···O(4)[g]	0.80(3)	2.69(3)	3.469(3)	164 (3)
C(4)−H(4)···O(5)[g]	0.80(3)	2.80(3)	3.480(3)	145(3)
C(18)−H(18)···O(6)[g]	0.85(3)	2.93(3)	3.681(4)	149 (3)
C(11)−H(11)···O(6)[h]	0.91(3)	2.67(3)	3.489(4)	152(3)
C(25)−H(25)···O(9)[i]	0.9 (5)	2.99(4)	3.850(4)	152(3)
O(10)−H(10B)···O(4)[j]	0.78(4)	2.01(4)	2.774(3)	170 (4)
O(10)−H(10A)···N(1)[k]	0.62(3)	2.23(3)	2.824(3)	164(4)
		6		
O(3)−H(3A)···O(1)	0.79(5)	1.85(5)	2.565(3)	150 (5)
O(7) −H(7A)···N(3)	0.81(5)	2.08(5)	2.869(4)	167(5)
O(8)−H(8A)···O(2)	0.85(5)	1.97(5)	2.789(4)	162(5)
O(6)−H(6A)···O(4)[l]	0.85(4)	1.72(4)	2.511(3)	153(5)
O(9)−H(9B)···O(10)[l]	0.79(4)	2.09(4)	2.859(4)	166(4)
O(8)−H(8B)···O(10)[l]	0.82(5)	2.26(5)	2.984(4)	149(5)
O(9)−H(9A)···N(1)[l]	0.824(5)	1.93(5)	2.739(4)	168(5)
O(7)−H(7B)···O(9)[m]	0.805(5)	2.14(5)	2.942(4)	174(4)
O(10)−H(10A)···O(2)[n]	0.827(4)	1.96(4)	2.778(3)	173(5)
O(10)−H(10B)···N(2)[o]	0.771(5)	2.13(5)	2.877(4)	163(5)

[a] Equivalent positions: $-x+2, -y, -z+1$. [b] Equivalent positions: $-x+1, -y, -z+1$. [c] Equivalent positions: $x-1, +y+1, +z$. [d] Equivalent positions: $x, +y-1, +z+1$. [e] Equivalent positions: $-x+1, -y+1, -z+1$. [f] Equivalent positions: $-x, -y+1, -z+1$. [g] Equivalent positions: $x+1, +y, +z$. [h] Equivalent positions: $-x, -y+1, -z$. [i] Equivalent positions: $x, +y-1, +z$. [j] Equivalent positions: $x, +y+1, +z$. [k] Equivalent positions: $-x+1, -y+1, -z$. [l] Equivalent positions: $-x+1, -y+1, -z+1$. [m] Equivalent positions: $-x+2, -y+1, -z+1$. [n] Equivalent positions: $x-1, +y+1, +z$. [o] Equivalent positions: $-x+1, -y+1, -z$.

two water molecules from the neighboring barium ions in the Ba_2 unit. The third water molecule forms intramolecular hydrogen bonds with the uncoordinated carboxylate oxygen atom O(2). It also forms a hydrogen bond with uncoordinated water oxygen O(10).

The 4bpy in **6** is not coordinated to the metal, and the chemical interactions involving this ligand are the same as those in **5**. There are three molecules of bipyridine for each Ba_2 unit. Two molecules are held near each barium center, using O−H···N hydrogen bonds (O(9)−H(9A)···N(1) and O(10)−H(10B)···N(2)) with coordinated water molecules and noncoordinated water molecules. The third one is held in-between the layers of one-dimensional chains and is also held by a hydrogen bond, with a coordinated water molecule (O(7)−H(7A)···N(3)) (Table 2). The presence of a large number of inter- and intramolecular hydrogen bonds in **6** gives rise to a three-dimensional supramolecular architecture, similar to that found in **5** (see the Supporting Information). All the Ba−O bond lengths around the metal center are different and range from 2.687(2) to 2.830(3) Å. The longer distances are those arising from coordinated water molecules, and the shortest distance is due to the bridging carboxylate oxygen atom.

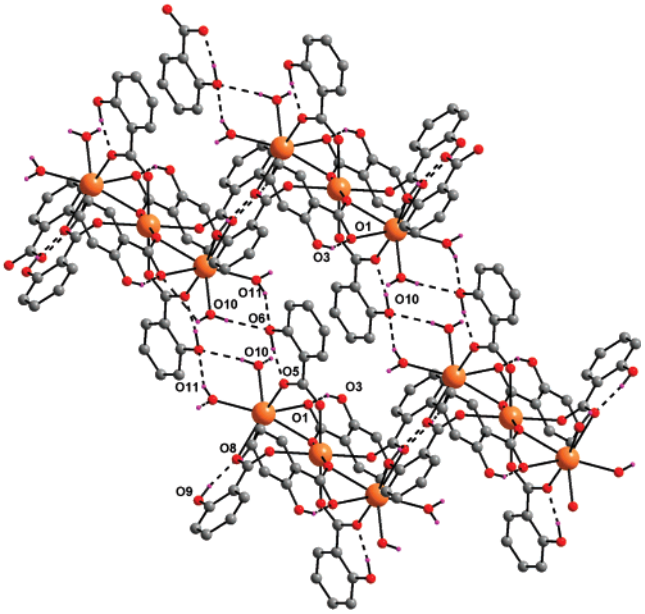

Figure 11. Hydrogen-bonding pattern in **4**.

Powder X-ray Diffraction (PXRD) Studies. The PXRD of bulk samples of **1**−**6** resulted in diffraction patterns that are indicative of the highly crystalline nature of the samples. Furthermore, it has been established that the PXRD pattern simulated from the single-crystal diffraction data of all samples match well with the experimentally measured PXRD profiles for the bulk samples obtained directly from the reaction mixture (see the Supporting Information). In the case of **4**, additional peaks were observed, probably due to presence of a second product, $[Ca(SA)_2(4bpy)_2(H_2O)_2]_n$, in the bulk sample.[45]

Thermal Decomposition Studies. Thermal analyses of complexes **1**−**6** have been carried out to establish the presence of water molecules and to derive the information to study the bulk decomposition to produce inorganic oxide/carbonate materials. The thermogravimetric analysis (TGA) profiles of compounds **1**−**3** do not show any weight loss up to 200 °C, indicating the absence of any coordinated or lattice water molecules, while those of **4**−**6** show a weight loss at temperatures as low as 38−195 °C, thus confirming the presence of coordinated/lattice water molecules. The TGA profiles of compounds **4**−**6** show a weight loss corresponding to the loss of four water molecules each. For phen complexes **1**−**3**, the major weight losses which occur around 200−300 °C correspond to the loss of the organic moieties, while for 4bpy derivatives **4**−**6**, the decomposition of aromatic moieties takes place at a higher temperature (300−580 °C). In all the cases, the final decomposition products are either the respective metal oxides or carbonates. While the decomposition for phenanthroline complexes is complete

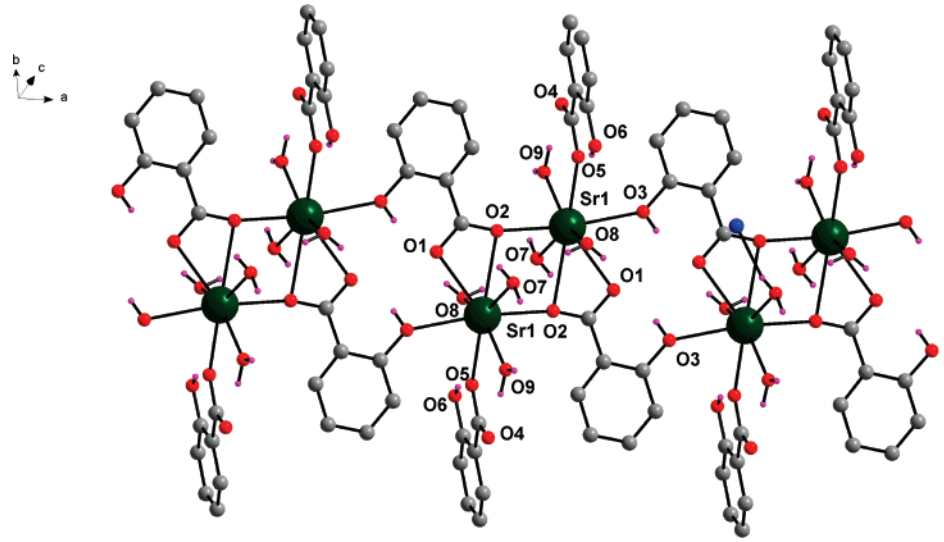

Figure 12. Polymeric chain in **5**. (lattice 4bpy units and water are not shown). Selected bond distances (Å) and angles (deg): Sr(1)−O(2)#1 2.530(2), Sr(1)−O(5)#1 2.550(2), Sr(1)−O(9) 2.551(2), Sr(1)−O(1) 2.580(2), Sr(1)−O(8) 2.607(2), Sr(1)−O(7) 2.626(2), Sr(1)−O(3)#2 2.688(2), Sr(1)−O(2) 2.823(2); O(2)#1−Sr(1)−O(5)#1 89.95(6), O(2)#1−Sr(1)−O(9) 91.76(6), O(5)#1−Sr(1)−O(9) 71.99(6), O(2)#1−Sr(1)−O(1) 122.76(5), O(5)#1−Sr(1)−O(1) 134.22(6), O(9)−Sr(1)−O(1) 130.24(6), O(2)#1−Sr(1)−O(8) 79.58(7), O(5)#1−Sr(1)−O(8) 75.96(6), O(9)−Sr(1)−O(8) 146.78(7), O(1)−Sr(1)−O(8) 79.54(6), O(2)#1−Sr(1)−O(7) 88.42(6), O(5)#1−Sr(1)−O(7) 139.76(6), O(9)−Sr(1)−O(7) 67.88(7), O(1)−Sr(1)−O(7) 77.67(6), O(8)−Sr(1)−O(7) 142.67(6), O(2)#1−Sr(1)−O(3)#2 172.12(5), O(5)#1−Sr(1)−O(3)#2 82.18(6), O(9)−Sr(1)−O(3)#2 85.48(6), O(1)−Sr(1)−O(3)#2 64.05(6), O(8)−Sr(1)−O(3)#2 98.74(7), O(7)−Sr(1)−O(3)#2 97.35(6), O(2)#1−Sr(1)−O(2) 74.79(6), O(5)#1−Sr(1)−O(2) 146.94(5), O(9)−Sr(1)−O(2) 136.18(6), O(1)−Sr(1)−O(2) 48.15(5), O(8)−Sr(1)−O(2) 72.56(6), O(7)−Sr(1)−O(2) 70.19(6), O(3)#2−Sr(1)−O(2) 112.19(5). Symmetry transformations used to generate equivalent atoms: #1, $-x$, $-y+1$, $-z+1$; #2, $-x+1$, $-y+1$, $-z+1$.

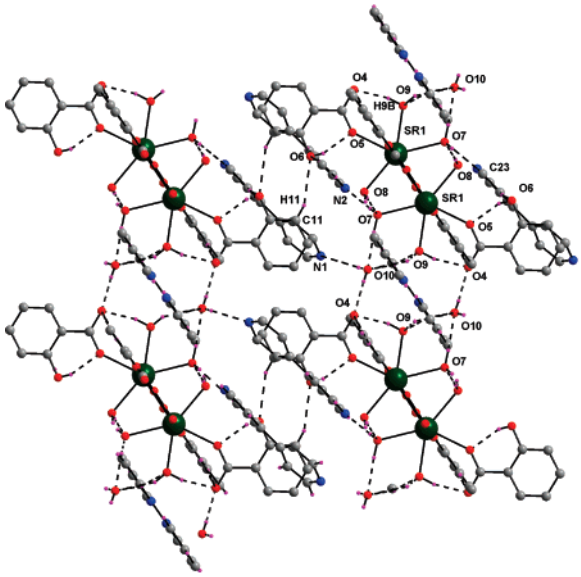

Figure 13. Formation of hydrogen bonds in **5**.

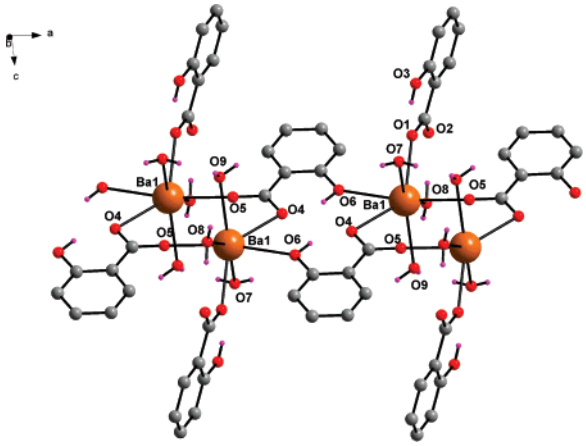

Figure 14. Molecular structure of **6** (the hydrogen atoms on the aromatic ring, nonbonded ′4bpy, and water molecules are omitted for clarity). Selected bond distances (Å) and angles (deg): Ba(1)−O(5) 2.687(2), Ba(1)−O(1) 2.706(2), Ba(1)−O(4) 2.743(2), Ba(1)−O(8) 2.768(3), Ba(1)−O(7) 2.815(3), Ba(1)−O(6) 2.824(2), Ba(1)−O(9) 2.830(3); O(5)−Ba(1)−O(1) 90.44(6), O(5)−Ba(1)−O(4) 122.86(6), O(1)−Ba(1)−O(4) 130.86(7), O(5)−Ba(1)−O(8) 92.96(7), O(1)−Ba(1)−O(8) 72.06(8), O(4)−Ba(1)−O(8) 132.09(8), O(5)−Ba(1)−O(7) 76.94(8), O(1)−Ba(1)−O(7) 77.42(7), O(4)−Ba(1)−O(7) 76.82(7), O(8)−Ba(1)−O(7) 147.76(8), O(5)−Ba(1)−O(6) 170.95(7), O(1)−Ba(1)−O(6) 80.59(6), O(4)−Ba(1)−O(6) 63.63(6), O(8)−Ba(1)−O(6) 85.48(7), O(7)−Ba(1)−O(6) 99.72(8), O(5)−Ba(1)−O(9) 90.57(7), O(1)−Ba(1)−O(9) 138.65(7), O(4)−Ba(1)−O(9) 81.08(7), O(8)−Ba(1)−O(9) 66.61(8), O(7)−Ba(1)−O(9) 142.55(7), O(6)−Ba(1)−O(9) 96.96(7).

by around 500−600 °C, the bipyridine complexes form the oxide materials only at around 700 °C.

Structural Chemistry of Calcium. Since calcium plays an important role in the structural biochemistry of almost all living organisms, the nature as well as the consequence of ligand binding of calcium needs special attention compared with other group 2 ions. An analysis of the coordination number and geometries of calcium in its complexes provides information which is helpful in the derivation of the action of biomolecules. The CSD and PDB databases have been used before for the analysis of calcium-containing complexes and biomolecules.[29,30] However, by taking into consideration that several new compounds and new coordination environments have been realized in the last 5 years, we have undertaken a detailed analysis of calcium-containing complexes in the literature as available in the November 2006 version of the CSD.

A total of 987 crystal structures containing calcium have been deposited in the CSD, of which 644 contain either O or N as donor atoms. Since our interest is to investigate the coordination environments of calcium in its carboxylate

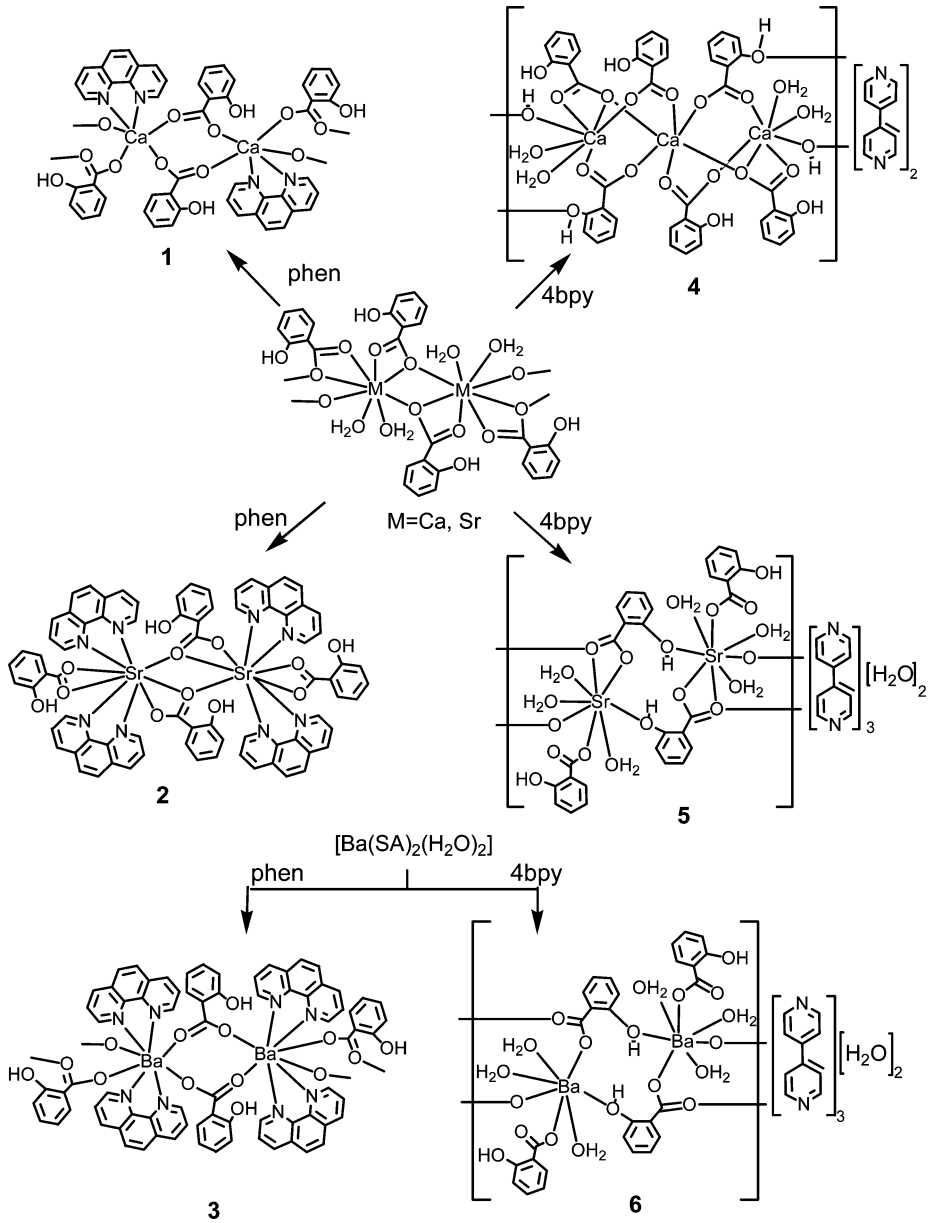

Figure 15. Schematic representation of the salicylate precursor complexes and the compounds **1**−**6** derived from them.

complexes, our analysis is limited to only those in which calcium is coordinated to a carboxylate group. There are 131 crystal structures in this category with 225 calcium binding sites. It is observed that although calcium forms coordination number as low as three, it prefers to have coordination numbers of six, seven, and eight in most of its carboxylate complexes, of which eight is the most preferred. Thus, out of the 225 binding sites, a total of 34 sites (15%) are found to have coordination numbers of six and 63 (28%) have a coordination number of seven, while 117 binding sites (52%) account for a coordination number of eight. Entries containing nine-coordinated calcium comprise of only 4% (nine binding sites) of the total calcium carboxylates. Only one crystal structure (HIFLIR) was found in which calcium has 10 and/or 11 coordination numbers.

Out of the total 131 crystal structures for calcium carboxylates, only 17 contain at least one nitrogen atom in the coordination sphere. Interestingly, there are no reports of calcium carboxylates in the CSD in which calcium is bonded to phen or 2,2′-bipyridine. In the only example where the calcium carboxylate complex contains 4bpy ligand (PARHAS), the 4bpy ligand is not coordinated to the metal, as in complexes **4**−**6**. A similar compound with 1,2-bis(4-pyridyl)-ethane has also been found in the CSD (PARHEW). The number and percentages of calcium binding sites (from the CSD) exhibiting different coordination numbers in its carboxylate complexes and the corresponding refcodes are given in the Supporting Information.

Conclusions

Our investigations on alkaline-earth metal salicylates, in the presence of two kinds of pyridinic auxiliaries (phen and 4bpy), have given rise to a variety of structural variations. The notable difference between phen complexes and 4bpy complexes is that, in the former case, phen occupies the coordination sphere of the metal in all three cases, while

Table 3. A Comparison of Structural Features in Compounds **1**−**6** with Precursors[a]

complex	cryst syst	space group	nuclearity	metal ion coordination number	coordination geometry around M ion	role of carboxylate ion
$[Ca(SA)_2(OH_2)_2]_n$ (**A**)	monoclinic	*C*2/*c*	polymer	eight	square antiprism	tridentate chelating
$[Ca(SA)_2(phen)]_n$ (**1**)	orthorhombic	*Pnab*	polymer	six	octahedral	bidentate bridging
$\{Ca_3(SA)_6(H_2O)_4](4bpy)_2\}_n$ (**4**)	triclinic	$P\bar{1}$	polymer	six and seven	octahedral/pentagonal bipyramidal	bidentate/tridentate bridging via carboxylate/phenolic
$[Sr(SA)_2(OH_2)_2]_n$	monoclinic	*C*2/*c*	polymer	eight	square antiprism	tridentate chelating
$[Sr_2(SA)_4(phen)_4]$ (**2**)	triclinic	*P*1	dimer	nine	monocapped square antiprismatic	chelating bidentate as well as tridentate
$[Sr(SA)_2(H_2O)_3]_n(4bpy)_{1.5}$-$(H_2O)n$ (**5**)	triclinic	$P\bar{1}$	polymer	eight	monocapped pentagonal bipyramidal	mono-/tetradentate via carboxylate as well as phenolic
$[Ba(SA)_2(phen)_2]_n$ (**3**)	monoclinic	*C*2/*c*	polymer	eight	bicapped octahedral	bidentate chelating
$[Ba(SA)_2(4bpy)_{1.5}(H_2O)_4]_n$ (**6**)	triclinic	$P\bar{1}$	polymer	seven	pentagonal bipyramidal geometry	mono-/tridentate via carboxylate and phenolic Continued

complex	hydrogen bond distinctive features	M−O bond lengths (Å)	M−N bond lengths (Å)	ref
$[Ca(SA)_2(OH_2)_2]_n$	O−H···O	2.379 to 2.632		15
$[Ca(SA)_2(phen)]_n$ (**1**)	O−H···O as well as C−H···O	2.245 and 2.363	2.5052	this work
$\{Ca_3(SA)_6(H_2O)_4](4bpy)_2\}_n$ (**4**)	O−H···O, C−H···O, and O−H···N	2.280(1) to 2.539(1)		this work
$[Sr(SA)_2(OH_2)_2]_n$ (**B**)	O−H···O	2.517 to 2.753		15
$[Sr_2(SA)_4(phen)_4]$ (**2**)	O−H···O and C−H···O	2.609(2) to 2.680(2)	2.738(2) to 2.824(2)	this work
$[Sr(SA)_2(H_2O)_3]_n(4bpy)_{1.5}$-$(H_2O)n$ (**5**)	O−H···O, C−H···O, and O−H···N	2.530(2) to 2.823(2)		this work
$[Ba(SA)_2(phen)_2]_n$ (**3**)	O−H···O and C−H···O	2.668(2) to 2.995(3)	2.927(9) to 2.995(1)	this work
$[Ba(SA)_2(4bpy)_{1.5}(H_2O)_4]_n$ (**6**)	O−H···O, C−H···O, and O−H···N	2.687(2) to 2.824(2)		this work

[a] All the polyhedral arrangements around the metal are highly distorted from normal.

4bpy is not coordinated to the metal in all the examples. However, the structures of the resulting metal complexes have shown considerable difference when compared with the metal salicylate complex formed in the absence of ancillary amines (Figure 15). For example, the presence of the ancillary amine changes the denticity of the carboxylate ligand, which in turn, alters the coordination environment around the metal center. The phen ligand changes the denticity of the ligand by chelation to the metal center, while the 4bpy ligand changes it even without metal coordination. In all the compounds, except **1** and **3**, the salicylate ligands exhibit more than one kind of binding mode. In **1** and **3**, the salicylate ligand is bridging bidentate, which is different than that found in the corresponding precursor complex (bridging tridentate). Thus, the phen ligand decreases the denticity of the salicylate ligand in **1** and **3**, while for Sr complex **2**, bi- and tridentate ligands are observed. The presence of 4bpy ligand, on the other hand, gives rise to more interesting properties of the salicylate ligand. Although the Sr and Ba derivatives (**5** and **6**) contain a monodentate salicylate ligand each, it is observed that in general the denticity properties of carboxylate ligands increase. The calcium derivative **4** has three types of carboxylate ligand, a bidentate bridging ligand and two tridentate bridging ligands. Among the two tridentate ligands, one uses carboxylate oxygens and other one uses carboxylate and phenolic oxygen atoms for metal binding. The most interesting behavior is exhibited by the phenolic group: for phenanthroline complexes (**1**−**3**), the phenolic group is involved only in the formation of hydrogen bonding. On the other hand, for bipyridine complexes, the phenolic group is involved in metal coordination as well as hydrogen-bond formation and thus helps to extend the polymeric framework.

The third property arising as a result of amine incorporation is that the molecular structures of phenanthroline complexes **1**−**3** do not have any coordinated water molecules, while those of bipyridine complexes crystallize with coordinated/noncoordinated water molecules, which may enter into various inter-/intramolecular hydrogen bonding configurations. The O−H···O hydrogen bonding between the ligands and the water molecules is of particular note, as this has marked influence on the solubility properties of the complexes. While **1**−**3** are only sparingly soluble in water, complexes **4**−**6** are readily soluble in water at room temperature (RT). A comparison of the structural features in **1**−**6** with those of the parent metal salicylates is given in Table 3.

Experimental Section

Instruments and Methods. The melting points were measured in glass capillaries and are reported uncorrected. Elemental analyses are performed on a Thermoquest Flash EA 1112 series CHNS analyzer. Infrared spectra were recorded on a Perkin-Elmer Spectrum One spectrometer as KBr diluted thin plates in the solid state. The UV−vis absorption and fluorescence spectra of the complexes were recorded at RT using a JASCO V-570 UV/vis/NIR spectrophotometer and a Perkin-Elmer LS 55 Luminescence spectrophotometer, respectively. For absorption and emission measurements, spectrophotometric grade methanol was used as solvent. The fluorescence lifetime measurements were carried out at IIT Bombay, using TCSPC method on a HORIBA Jobin Yvon IBH Fluorocube equipped with a nanoLED source. TGA and

Table 4. Crystallographic Cell Parameters and Experimental Details of X-ray Intensity Data Collection for Metal Complexes

	1	2	3	4	5	6
identification code	rm152c	mur106	rm186a	newrm055	newrm072	newrm063
empirical formula	$C_{26}H_{18}CaN_2O_6$	$C_{38}H_{26}N_4O_6Sr$	$C_{38}H_{26}BaN_4O_6$	$C_{62}H_{54}Ca_3N_4O_{22}$	$C_{29}H_{30}N_3O_{10}Sr$	$C_{29}H_{30}BaN_3O_{10}$
fw	494.50	722.25	771.97	1327.33	668.18	717.90
T, K	293(2)	133(2)	293(2)	150(2) K	151(2)	150(2)
λ, Å	0.71073	0.71073	0.71073	0.71073	0.71073	0.71073
crystal system	orthorhombic	triclinic	monoclinic	triclinic	triclinic	triclinic
space group	*Pnab*	$P\bar{1}$	*C*2/*c*	$P\bar{1}$	$P\bar{1}$	$P\bar{1}$
a, Å	7.6730(11)	10.918(2)	14.399(1)	10.199(1)	9.226(1)	9.4822(4)
b, Å	12.5220(7)	12.548(3	22.178(2)	11.988(3)	11.893(2)	12.147(2)
c, Å	23.897(1)	13.458(3)	10.233(1)	14.257(3)	13.354(4)	13.216(2)
α, (deg)	90	107.35(3)	90	67.05(2)	87.998(17)	88.160
β, (deg)	90	113.53(3)	99.222(8	77.69(2)	82.001(16)	83.952(8)
γ, (deg)	90	97.20(3)	90	74.00(2)	82.509(11)	81.449(8)
V, Å^3	2296.1(4)	1549.3(5)	3225.5(5)	1532.0(5)	1438.3(5)	1496.7(3)
Z	4	2	4	1	2	2
ρ (calcd), Mg/m^3	1.431	1.548	1.590	1.439	1.543	1.593
abs coeff, mm^{-1}	0.320	1.798	1.287	0.353	1.938	1.388
F(000)	1024	736	1544	690	686	722
crystal size, mm^3	0.40 × 0.15 × 0.10	0.30 × 0.30 × 0.20	0.35 × 0.30 × 0.25	0.35 × 0.30 × 0.30	0.33 × 0.28 × 0.17	0.42 × 0.36 × 0.32
θ range	1.70 to 24.97	1.77 to 24.78	1.70 to 27.47	3.03 to 25.00	3.00 to 25.00	2.95 to 25.00
total reflns	1994	25 348	3907	16 845	14 661	13 808
unique reflns	1994	5283	3701	5375	5021	5263
goodness of fit on F^2	0.982	1.050	1.057	1.129	1.050	1.099
R_1 [$I > 2\sigma(I)$]	0.0517	0.0243	0.0335	0.0299	0.0301	0.0259
R_2 [$I > 2\sigma(I)$]	0.0944	0.0599	0.0747	0.0742	0.0810	0.0632
largest peak, e Å^3	0.238	0.742	0.750	0.243	0.759	0.792
largest hole, e Å^3	−0.328	−0.275	−0.953	−0.228	−0.446	−1.306

differential thermal analysis were carried out on a Perkin-Elmer Pyris/ Diamond thermal analysis system under a stream of nitrogen gas. The ^{1}H and ^{13}C NMR spectra were recorded on a Varian 300 MHz instrument using Me_4Si as a reference. X-ray powder diffraction data were obtained with a Philips X'Pert PRO X-ray Diffraction System using monochromated Cu Kα1 radiation (λ =1.5406 Å).

Single-Crystal X-ray Diffraction Studies. The intensity data collection for compounds **1** and **3** has been carried out on a Nonius MACH3 diffractometer, for **2** on a Siemens STOE AED2 four-circle diffractometer, and for **4**−**6** on an Oxford Diffraction XCalibur-S diffractometer, equipped with a CCD system. The unit cell dimensions were determined using approximately 25 well-centered and well-separated high angle reflections in each case. Intensity data collection and cell determination protocols were carried out using a graphite-monochromatized Mo K_α radiation (λ = 0.71073 Å) in all the three diffractometers. The resultant intensity data have been corrected for Lorentz polarization and absorption effects, wherever necessary. Structure solution for each of the compounds was obtained using direct methods as implemented in WinGX platform (*SHELXS-97*)[57] and refined using full-matrix least-square methods on F^2 using *SHELXL-97*.[57] The hydrogen atoms were either located in the successive difference maps or were geometrically fixed and refined using a riding model. All non-hydrogen atoms were refined anisotropically. A summary of the crystal data, structure solution and refinement are given in Table 4.

Database Analyses. The Cambridge Structural Database (CSD) was searched using QUEST for all published crystal structures containing divalent calcium ions in which calcium is bonded to one or more carboxylate groups.[58] We limited our search to those for which crystallographic *R* factors is less than 0.10. This file obtained from the CSD was then analyzed for different coordination environments around calcium ion, and compared with the structures reported in this article.

Synthesis. $[Ca(SA)_2(phen)]_n$ (1). A solution of 1,10-phenanthroline (phen) (0.2703 g, 1.5 mmol) in MeOH (20 mL) was added slowly along the wall of the beaker to a solution of $[Ca(SA)_2(OH_2)_2]$ (0.1772 g, 0.5 mmol) in MeOH/H_2O mixture (20 mL, 1:1) without causing any disturbance. The resultant solution was kept undisturbed for recrystallization at RT. Colorless needle-shaped single crystals were observed to form overnight. Mp: >200 °C. Yield: 0.160 g, 64% (based on $[Ca(SA)_2(OH_2)_2]$). Anal. Calcd for $CaC_{26}H_{18}O_6N_2$: C, 63.1; H, 3.7; N, 5.7. Found: C, 62.4; H, 3.4; N, 5.5. IR (KBr, cm^{-1}): 3444 (w), 3060 (w), 1654 (s), 1618 (s), 1596 (s), 1488 (s), 1467 (m), 1391 (s), 1358 (s), 1256 (m), 1207 (w), 1148 (m), 1030 (w), 864 (s), 846 (s), 760 (s). ^{1}H NMR (DMSO-d_6, 400 MHz): δ 6.62−6.66 (m, 2H, H_g), ($^3J_{HH}$ = 7.32 Hz, $^4J_{HH}$= 1.22 Hz), 6.65−6.67 (d, 2H, H_e), ($^3J_{HH}$ = 7.94 Hz), 7.18 (m, 2H, H_f), ($^3J_{HH}$ = 7.94 Hz, $^4J_{HH}$ = 1.52 Hz), 7.72 (dd, 2H, H_h), ($^3J_{HH}$ = 7.94 Hz, $^4J_{HH}$ =1.83 Hz), 7.79 (dd, 2H, H_c), ($^3J_{HH}$ =7.96 Hz, $^4J_{HH}$ = 4.27 Hz), 8.01 (s, 2H, H_a), 8.51(dd, 2H, H_b), ($^3J_{HH}$ =7.96 Hz, $^4J_{HH}$ = 1.83 Hz), 9.12 (s, 2H, H_d), 15.52 (s, 2H, OH) ppm. ^{13}C NMR (DMSO-d_6, 400 MHz): δ 115.99 (C_j), 116.6 (C_h), 119.6 (C_i), 123.5 (C_d), 127.0 (C_a), 128.5 (C_b), 130.2 (C_k), 132.1(C_m), 136.6 (C_c), 145.3 (C_f), 150.2 (C_e),162.3 (C_i), 172.9 (C_g) ppm. UV−vis (CH_3OH, nm, ϵ, cm^{-1} M^{-1}): 207 (6.7 × 10^4), 229 (1.4 × 10^5), 262 (1.2 × 10^5). Fluorescence (λ_{ex} =262 nm, CH_3OH): 366 and 383 nm (emission); 271 and 295 nm (excitation). Fluorescence lifetime (τ, ns): 5.41.

$[Sr_2(SA)_4(phen)_4]$ (2). To a solution of $[Sr(SA)_2(OH_2)_2]_n$ (0.3978 g, 1 mmol) in MeOH (50 mL)/H_2O (20 mL) phen (0.1352 g, 0.75 mmol) was added, and the resulting solution was stirred 30 min, filtered, and the resulting solution was kept at RT for crystallization. Colorless diamond-shaped crystals were formed in several days. Mp: >200 °C. Yield: 0.309 g, 43% (based on $[Sr(SA)_2(OH_2)_2]_n$).

(57) (a) Sheldrick, G. M. *SHELXS-97. Program for Crystal Structure Solution;* University of Göttingen: Göttingen, Germany, 1997. (b) Sheldrick, G. M. *SHELXL-97. Program for Crystal Structure Refinement*; University of Göttingen: Göttingen, Germany, 1997.

(58) Allen, F. H.; Bellard, S.; Brice, M. D.; Cartwright, B. A.; Doubleday, A.; Higgs, H.; Hummelink, T.; Hummelink-Peters, G. G.; Kennard, O.; Motherwell, W. D. S.; Rodgers, J. R.; Watson, D. G. The Cambridge Crystallographic Data Centre: computer-based search, retrieval, analysis and display of information. *Acta Crystallogr*. **1979**, *B35*, 2331.

Anal. Calcd for $Sr_2C_{76}H_{52}O_{12}N_8$: C, 63.2; H, 3.6; N, 7.8. Found: C, 63.0; H, 3.7; N, 7.3. IR (KBr, cm^{-1}); 3435 (w), 1625 (m), 1592 (m), 1561 (m) 1513 (s), 1489 (s), 1459 (s), 1423 (m), 1394 (s), 1355 (s), 1257 (m), 1139 (m), 861 (s), 845 (s), 763 (s). ^{1}H NMR (DMSO, 400 MHz): δ 6.60−6.70 (m, 4H, H_e, H_g), ($^3J_{HH}$ = 7.70 Hz), 7.18 (m, 2H, H_f), ($^3J_{HH}$ = 7.67 Hz, $^4J_{HH}$ = 2.44 Hz), 7.70 (dd, 2H, H_h), ($^4J_{HH}$ = 1.83 Hz, $^3J_{HH}$ = 7.64 Hz), 7.8 (dd, 4H, H_c) ($^3J_{HH}$ = 8.07 Hz, $^4J_{HH}$ = 4.40 Hz), 8.02 (s, 4H, H_a), 8.52 (dd, 4H, H_b) ($^4J_{HH}$ = 1.46 Hz, $^3J_{HH}$ = 8.07 Hz), 9.12 (dd, 4H, H_d), ($^4J_{HH}$ = 1.47 Hz, $^3J_{HH}$ = 4.03 Hz), 15.41 (s, 4H, OH) ppm. UV−vis (CH_3-OH, nm): 208 (1.3 × 10^5), 229 (2.0 × 10^5), 264 (1.2 × 10^5). Fluorescence (λ_{ex} = 263 nm, CH_3OH): 366 and 383 nm (emission); 270 and 293 (excitation) nm. Fluorescence lifetime (τ, ns): 5.50.

[Ba(SA)$_2$(phen)$_2$]$_n$ (3). [Ba(SA)$_2$(OH$_2$)$_2$]$_n$ (0.4476 g, 1 mmol) was dissolved in H_2O/MeOH mixture (10/ 20 mL) and to the above solution phen (0.3604 g, 2 mmol) was added. The resulting solution was heated for 10 min on a water bath, filtered, and kept at RT for crystallization. Colorless diamond-shaped crystals were formed within few hours. Mp: >235−240 °C. Yield: 0.463 g (60% based on [Ba(SA)$_2$(OH$_2$)$_2$]$_n$). Anal. Calcd for $BaC_{38}H_{26}O_6N_4$: C, 59.1; H, 3.4; N, 7.3. Found: C, 58.8; H, 3.4; N, 6.4. IR (KBr, cm^{-1}); 3445 (w), 3067 (w), 1637 (s), 1623 (s), 1557 (s), 1566 (s), 1479 (s), 1457 (s), 1420 (s), 1377 (s), 1335 (s), 1251 (m), 856 (s), 848 (s), 761 (s). ^{1}H NMR (DMSO-d_6, 400 MHz): δ 6.60 (t, 2H, H_g) ($^3J_{HH}$ = 7.33 Hz), 6.62 (d, 2H, H_e) ($^3J_{HH}$= 8.8 Hz), 7.14 (m, 2H, H_f) ($^3J_{HH}$ =7.52 Hz, $^4J_{HH}$ = 2.20 Hz), 7.66 (dd, 2H, H_h) ($^4J_{HH}$ = 1.47 Hz, $^3J_{HH}$ = 7.33 Hz), 7.76 (dd, 2H, H_c), ($^3J_{HH}$ = 8.07 Hz, $^4J_{HH}$ = 4.40 Hz), 8.0(s, 4H, H_a), 8.51 (dd, 4H, H_b), ($^3J_{HH}$ = 8.07 Hz, $^4J_{HH}$ = 1.47 Hz), 9.11 (dd, 4H, H_d) ($^3J_{HH}$ = 4.40 Hz, $^4J_{HH}$ = 1.47 Hz) ppm. UV−vis (CH_3OH, nm, ϵ, cm^{-1} M^{-1}): 212 (1.5 × 10^5), 229 (2.03 × 10^5), 264 (1.94 × 10^5), Fluorescence (λ_{ex} = 262 nm, CH_3OH): 366 and 383 nm (emission); 271 and 292 nm (excitation). Fluorescence lifetime (τ, ns): 5.44.

Synthesis of Compounds 4−6. Compounds **4**−**6** were prepared using similar synthetic procedure starting from the corresponding metal carbonates MCO_3 (M = Ca (**4**), Sr (**5**), and Ba (**6**)). In a typical synthesis, the metal carbonates (2.5 mmol) were taken as a suspension in H_2O (40 mL) and SA−H (0.6906 g, 5 mmol) was added to this. The mixture was heated till the solution becomes clear and the effervescence stops completely. 4,4′-bipyridine (4bpy) (0.39 g, 2.5 mmol) was dissolved in MeOH (10 mL), and the former solution was filtered into this. The resulting solution was heated for 10 min on a water bath, filtered, and kept at RT for crystallization. X-ray quality crystals were obtained directly from the solution.

{[Ca$_3$(SA)$_6$(H$_2$O)$_4$](4bpy)$_2$}$_n$ (4). Mp: >260 °C. Yield: 0.354 g (32% based on $CaCO_3$). Anal. Calcd for $Ca_3C_{66}H_{54}O_{22}N_4$: C, 56.1; H, 4.1; N, 4.2. Found: C, 55.8; H, 4.0; N, 3.9. IR (KBr, cm^{-1}): 3532 (m), 1595 (s), 1489 (s), 1462 (s), 1396 (s), 1365 (m), 1341 (m), 1256 (m), 1143 (w), 762 (s). ^{1}H NMR (DMSO-d_6, 400 MHz): δ 6.64 (t, 2H, H_e), ($^3J_{HH}$ = 7.33 Hz), 6.66 (d, 2H, H_c) ($^3J_{HH}$ = 9.5 Hz), 7.19 (m, 6H, H_d), ($^3J_{HH}$ = 7.33 Hz, $^4J_{HH}$ = 1.47 Hz), 7.72 (dd, 6H, H_f), ($^4J_{HH}$ = 1.83, $^3J_{HH}$ = 7.69 Hz), 7.83 (dd, 8H, H_b), ($^3J_{HH}$ = 1.83 Hz, $^4J_{HH}$ = 4.77 Hz), 8.73 (dd, 8H, H_a), ($^3J_{HH}$ = 4.40 Hz, $^4J_{HH}$ = 1.47 Hz), 15.48 (s, 2H, OH) ppm. ^{13}C NMR (DMSO-d_6, 300 MHz): δ 114.71 (C_g), 116.49 (C_e), 116.59 (C_i), 120.53 (C_b), 129.27 (C_j), 131.74 (C_h), 144.69 (C_c), 148.49 (C_a), 159.96 (C_f), 174.99 (C_d) ppm. UV−vis (CH_3OH, nm, ϵ, cm^{-1}, M^{-1}): 206 (7.6 × 10^4), 234 (6.3 × 10^4), 302 (1.1 × 10^4). Fluorescence (λ_{ex} = 234 nm, CH_3OH): 401 and 297 nm. Fluorescence lifetime (τ, ns): 5.61.

{[Sr(SA)$_2$(H$_2$O)$_3$](4bpy)$_{1.5}$(H$_2$O)}$_n$ (5). Mp: >250 °C. Yield: 0.779 g, 53% (based on $SrCO_3$). Anal. Calcd for $SrC_{29}H_{30}O_{10}N_3$: C, 52.1; H, 4.5; N, 6.3. Found: C, 52.6; H, 3.9; N, 7.6. IR (KBr, cm^{-1}): 3424 (s), 3100 (s), 1689 (w), 1619 (s), 1595 (s), 1567 (s), 1484 (s), 1455 (s), 1408 (s), 1384 (s), 1346 (s), 1251 (s), 1216 (w), 870 (m), 803 (m), 762 (s). ^{1}H NMR (DMSO-d_6, 400 MHz): δ 6.65 (t, 2H, H_e), ($^3J_{HH}$ = 7.70 Hz), 6.67 (d, 2H, H_c), ($^3J_{HH}$ = 8.80 Hz), 7.18 (m, 2H, H_d), ($^3J_{HH}$ = 7.99 Hz, $^4J_{HH}$ = 1.83 Hz), 7.71 (dd, 2H, H_f), ($^4J_{HH}$ = 1.83 Hz, $^3J_{HH}$ = 7.70 Hz), 7.83 (dd, 6H, H_b) ($^3J_{HH}$ = 4.40 Hz, $^4J_{HH}$ = 1.47 Hz), 8.72 (dd, 6H, H_a) ($^3J_{HH}$ = 4.40 Hz, $^4J_{HH}$= 1.47 Hz), 15.35 (s, 2H, OH) ppm. UV−vis (CH_3-OH, nm, ϵ, cm^{-1}, M^{-1}): 207 (1.4 × 10^5), 234 (8.0 × 10^4), 300 (1.9 × 10^4). Fluorescence (λ_{ex} = 234 nm, CH_3OH): 397 and 296 nm. Fluorescence lifetime (τ, ns): 5.54.

{[Ba(SA)$_2$(H$_2$O)$_3$](4bpy)$_{1.5}$(H$_2$O)}$_n$ (6). Mp: 185−190 °C. Yield: 0.942 g, 56% (based on $BaCO_3$). Anal. Calcd for $BaC_{29}H_{30}O_{10}N_3$: C, 48.5; H, 4.2; N, 5.9. Found: C, 46.1; H, 4.4; N, 6.3. IR (KBr, cm^{-1}): 3399 (m), 1686 (w), 1618 (s), 1595 (s), 1567 (s), 1484 (s), 1455 (s), 1407 (s), 1388 (s), 1343 (m), 1302 (m), 1253 (s), 1216 (w), 866 (m), 803 (m), 760 (s). ^{1}H NMR (DMSO-d_6, 400 MHz): δ 6.63 (m, 4H, H_c, H_e), ($^3J_{HH}$ = 8.07 Hz, $^4J_{HH}$ = 1.47 Hz), 7.17 (m, 2H, H_d), ($^3J_{HH}$ = 7.14 Hz, $^4J_{HH}$ = 1.83 Hz), 7.69 (dd, 2H, H_f), ($^3J_{HH}$= 7.33 Hz, $^4J_{HH}$= 1.47 Hz), 7.83 (dd, 6H, H_b) ($^3J_{HH}$ = 2.20 Hz, $^4J_{HH}$ = 4.40 Hz), 8.72 (dd, 6H, H_a) ($^3J_{HH}$ = 4.40 Hz, $^4J_{HH}$ = 2.20 Hz), 15.67 (s, 2H, OH) ppm. UV−vis (CH_3OH, nm, ϵ, cm^{-1} M^{-1}): 207 (1.4 × 10^5), 234 (7.5 × 10^4), 300 (1.9 × 10^4). Fluorescence (λ_{ex} = 234 nm, CH_3OH): 399 and 296 nm. Fluorescence lifetime (τ, ns): 5.51.

Acknowledgment. The authors acknowledge the DST, New Delhi, for financial support in the form of a Swarnajayanthi fellowship (to R.M.). R.K. thanks the CSIR for a research fellowship. We acknowledge the National Single Crystal X-ray Diffraction Facility and SAIF at IIT-Bombay for single-crystal diffraction, analytical, and spectroscopic data. We thank Mr. S. Kuppuswamy for his help in COSY NMR studies, Mr. S. Shanmugan for his help in revising the manuscript, and the reviewers for their useful suggestions.

Supporting Information Available: Additional characterization data (PDF; 24 pp) and details of X-ray diffraction studies of compounds **1**−**6** (CIF-type Mercury file). This material is available free of charge via the Internet at http://pubs.acs.org.

IC700977W